HPC on particle accelerations at collisionless shocks

Yosuke Matsumoto
Department of Physics
Chiba University

Collaborators:
T. Amano & M. Hoshino (Univ. of Tokyo)
T. N. Kato (Hiroshima Univ.)

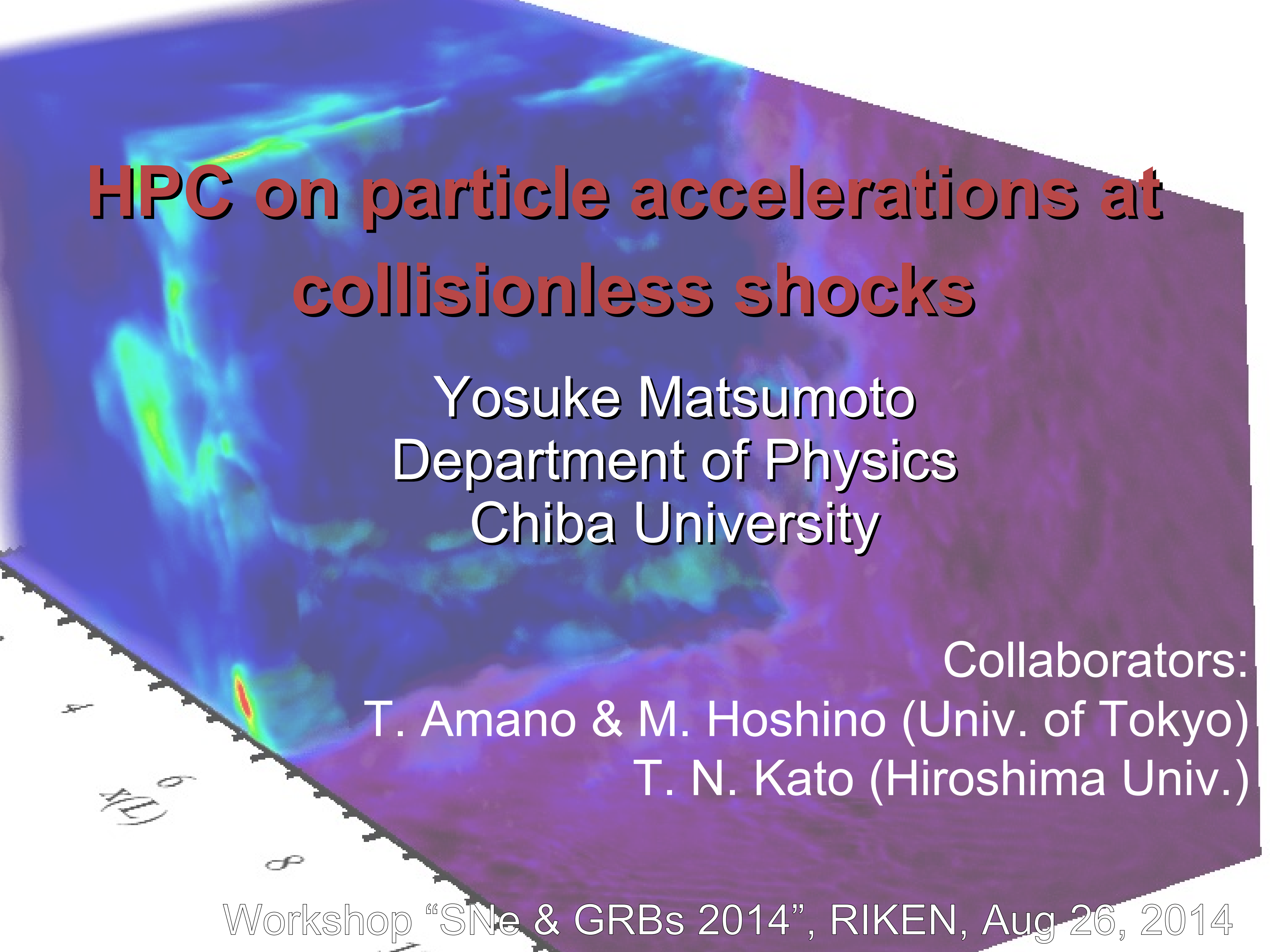

Workshop “SNe & GRBs 2014”, RIKEN, Aug 26, 2014

Collisionless shocks as particle accelerators

Planetary bow shocks

v_{sh}/c

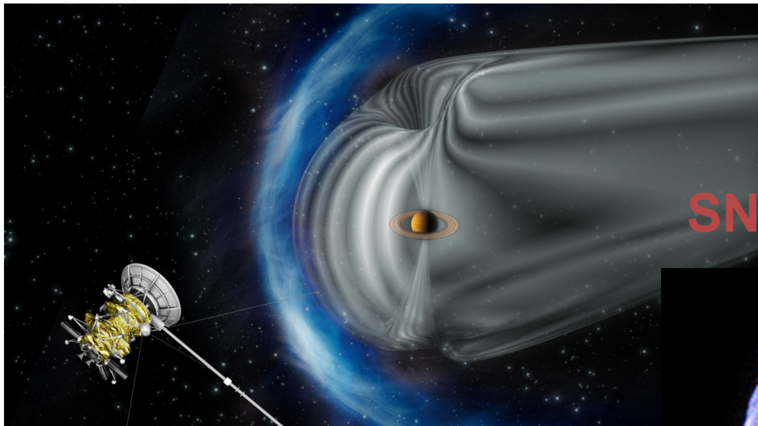

e.g., Masters+ '13

SNR shocks (M_A>100)

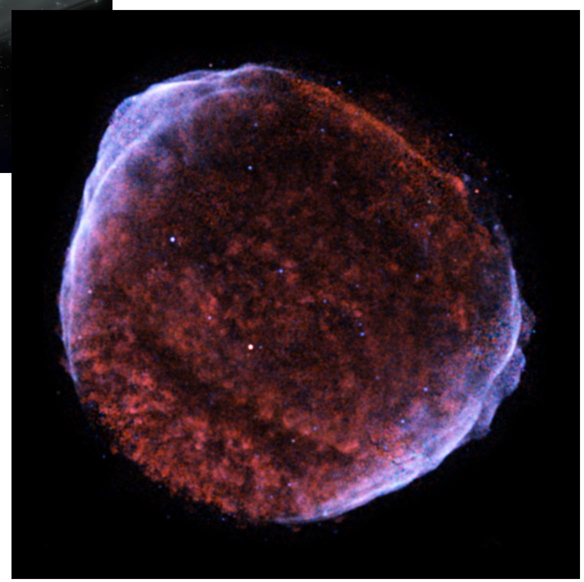

e.g., Bamba+ 03

GRBs, AGN jets (v_{sh} ~ c)

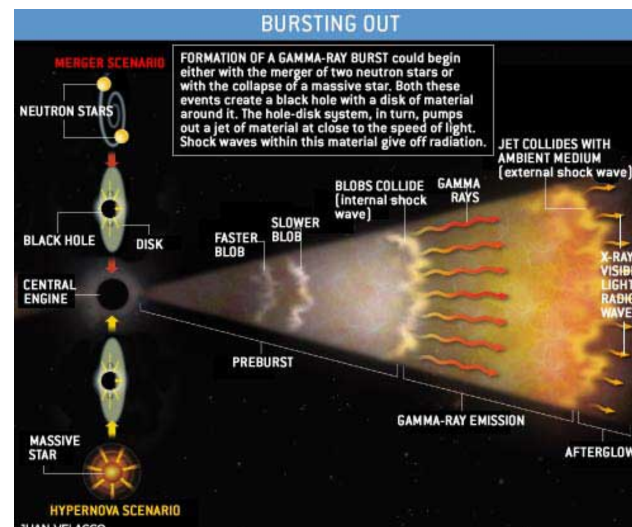

e.g., Meszaros '01

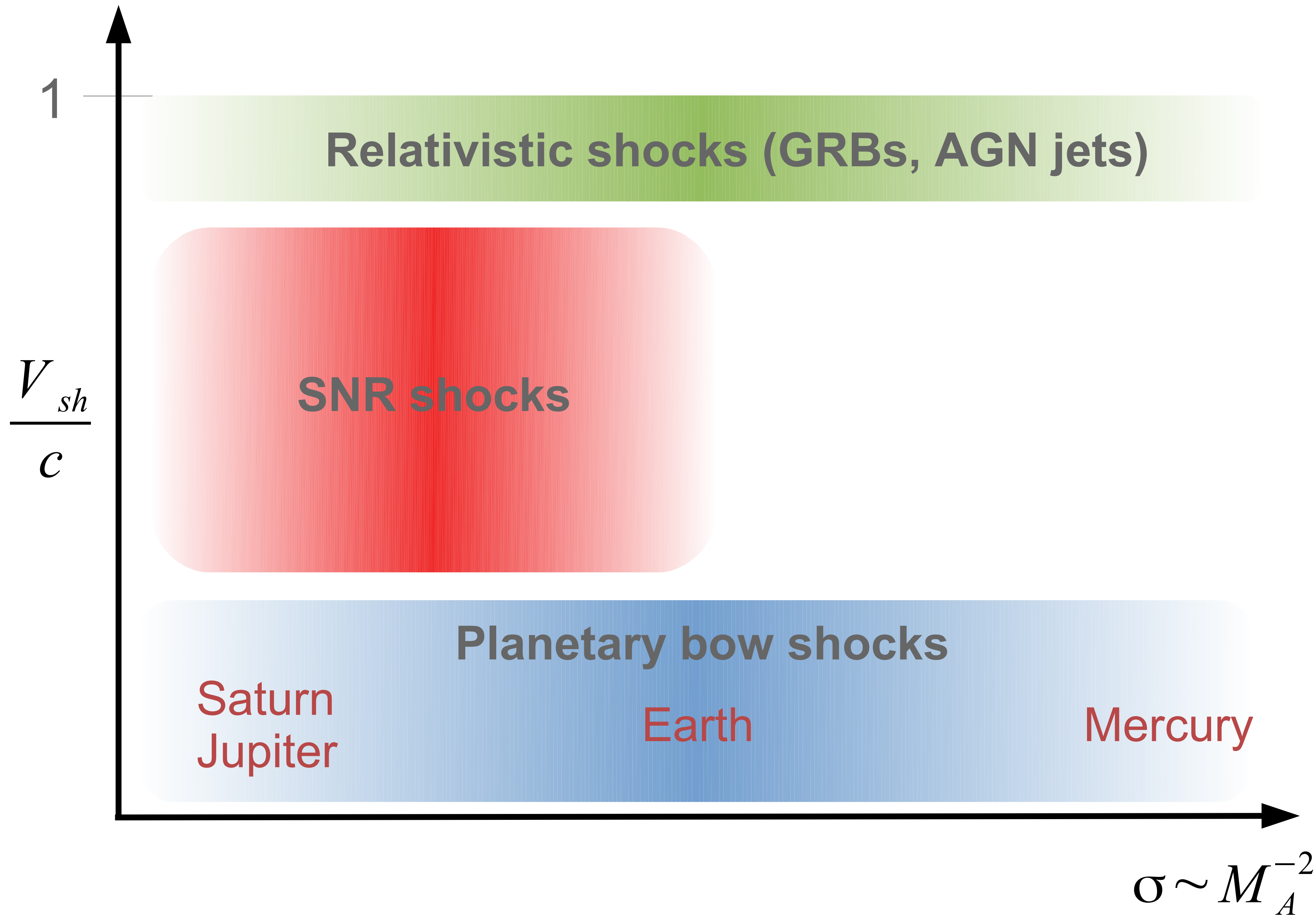
1
Relativistic shocks (GRBs, AGN jets)
SNR shocks
Planetary bow shocks
Saturn
Jupiter
Earth
Mercury
$\frac{V_{sh}}{c}$
$\sigma \sim M_A^{-2}$

Diffusive shock acceleration

head-on collisions with magnetic turbulence

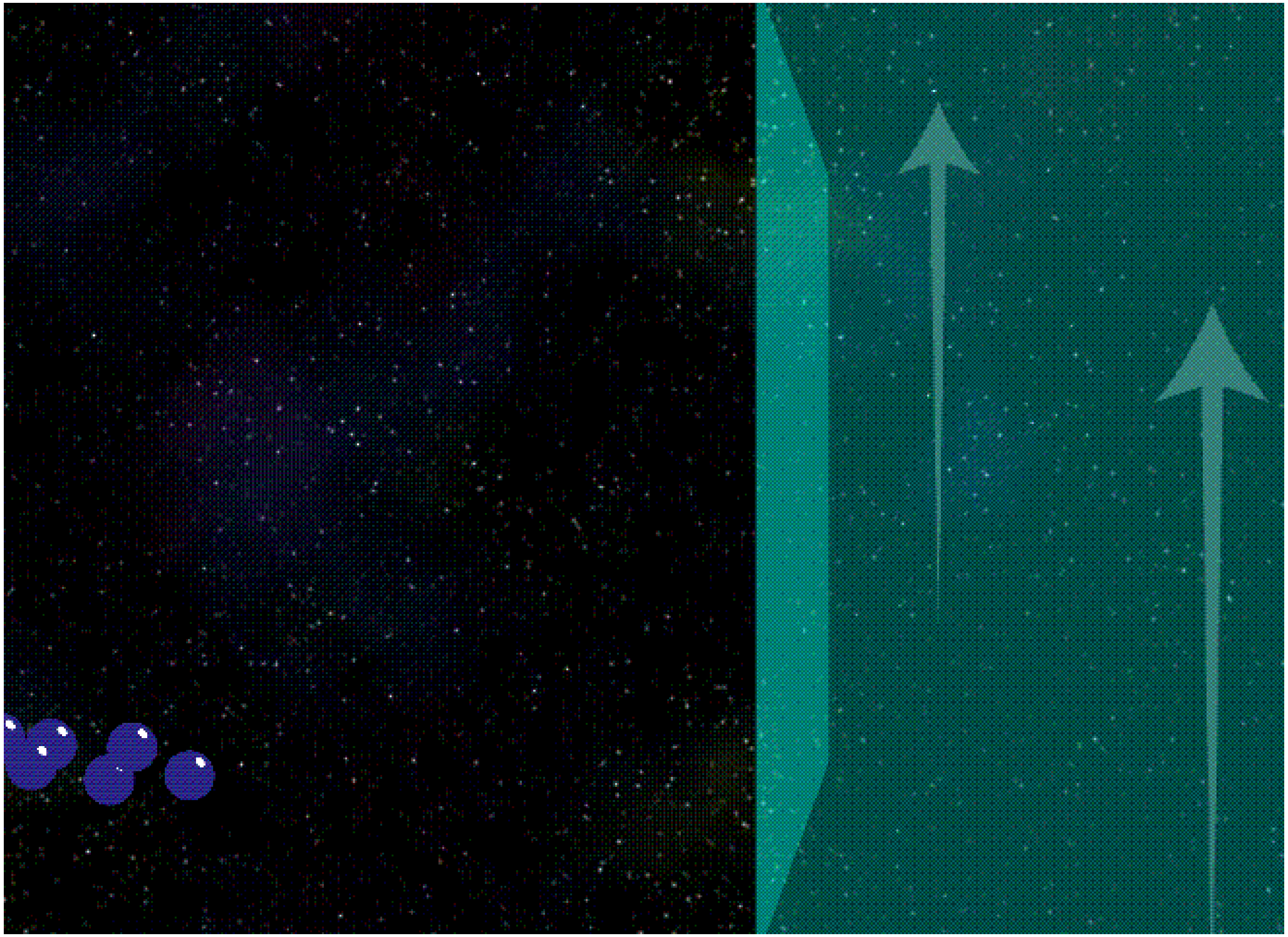

Coutesy of Irie-san@KEK

Theoretical issues

Injection

- Shock scale $L \sim \alpha\lambda_i >> r_{ge}$
- Thermal electrons are strongly magnetized
- $\gamma_e > \sim 10$ can be injected
- Pre-acclerations for electrons are necessary

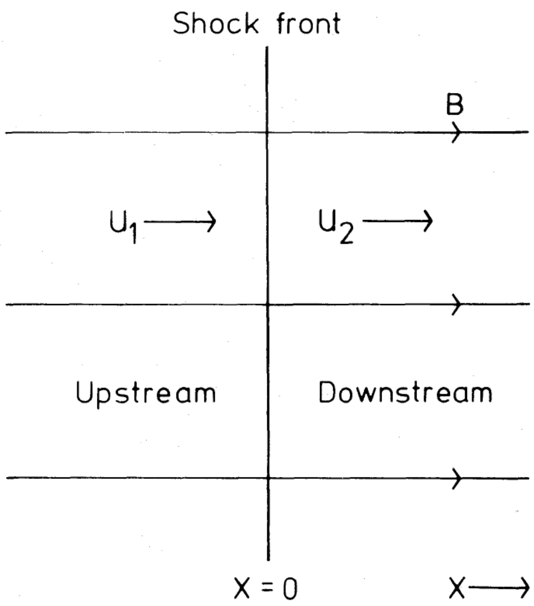

Bell, 1974

Scattering bodies

- Alfven waves – preferential in paralllel shocks
- magnetic clouds – found in perpendicular shocks (this work)
- magnetic field amplification (x ~100)

Super-critical (M_A> ~3) shock structures

“Reflected ions”

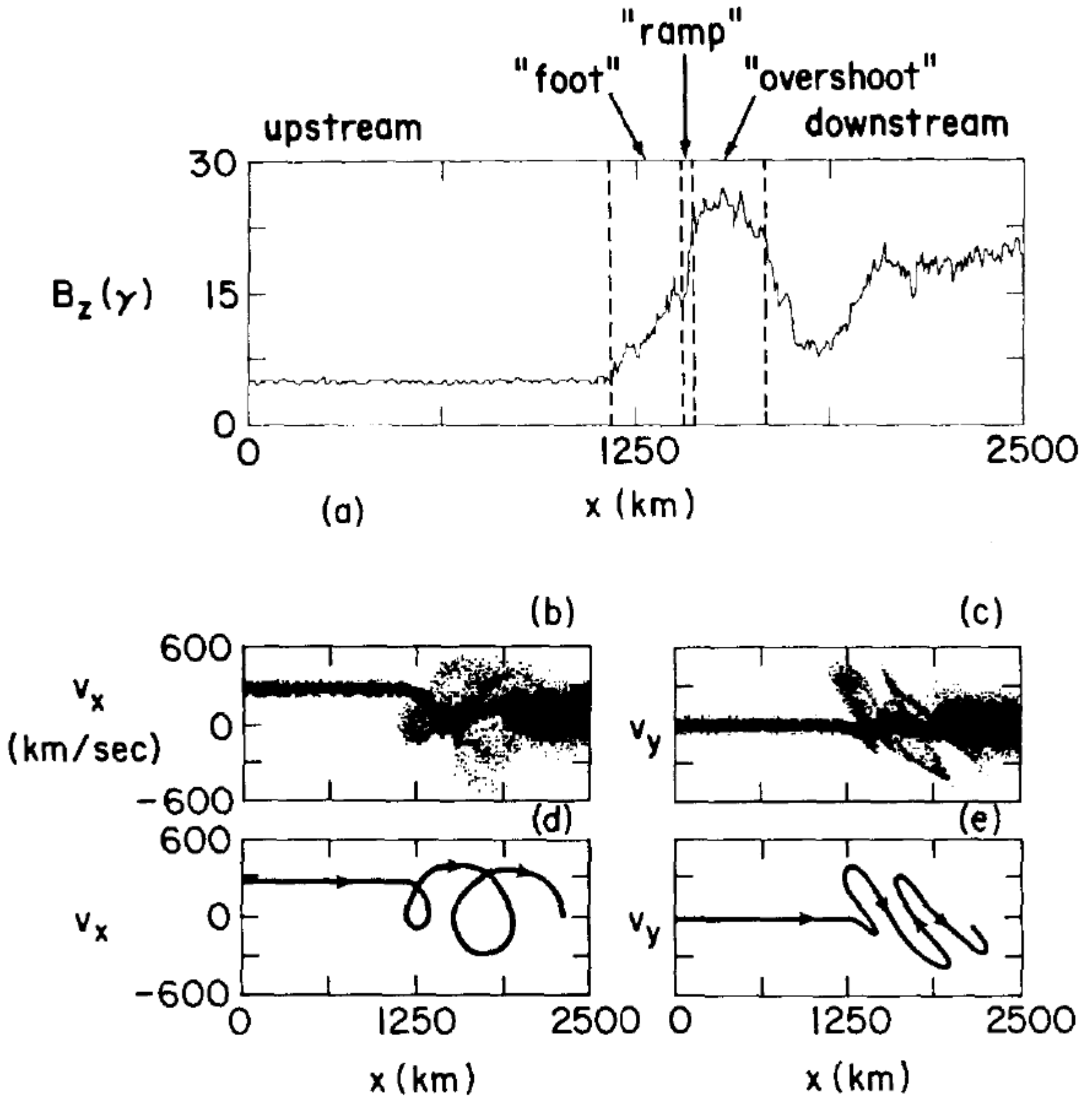

Leroy 82; Wu+ 84

Plasma kinetic instabilities in shock structures

Microinstabilities in the shock front region

Instability	Excitation by	Source of free energy	Direction of propagation
Ion-ion streaming instability	Reflected ions and transmitted ions	Relative streaming between the ion species	$(\mathbf{k}\cdot\mathbf{B}_0) = 90°$
Kinetic cross-field streaming instability	Reflected ions	Relative streaming between the reflected ions and the solar wind electrons	$0 < (\mathbf{k}\cdot\mathbf{B}_0) < 90°$ (In the coplanarity plane)
	Transmitted ions	Relative streaming between the transmitted ions and the electrons	$(\mathbf{k}\cdot\mathbf{B}_0) \leq 90°$ (In the coplanarity plane)
Lower-hybrid-drift instability	Reflected ions	(i) Relative cross-field drift between the reflected ions and the electrons (ii) Density gradient	$(\mathbf{k}\cdot\mathbf{B}_0) < 90°$ (Out of the coplanarity plane)
	Drifting electrons	(i) Relative cross-field drift between the electrons and the transmitted ions (ii) Density gradient	$(\mathbf{k}\cdot\mathbf{B}_0) < 90°$ (Out of the coplanarity plane)
Ion-acoustic instability	Transmitted ions	Relative streaming between the ion species and the electrons	$(\mathbf{k}\cdot\mathbf{B}_0) < 90°$ (Out of the coplanarity plane)
Electron-cyclotron drift instability	Drifting electrons	Electron drift relative to the solar wind ions	$(\mathbf{k}\cdot\mathbf{B}_0) \simeq 90°$ (Out of the coplanarity plane)
Whistler instability	Electrons	Electron thermal anisotropy $T_{e\perp} > T_{e\parallel}$	$(\mathbf{k}\cdot\mathbf{B}_0) \simeq 0°$

Microinstabilities in the shock front region (continued)

Instability	Nature of wave mode	Typical wavelength	Frequency and growth rate	Remarks
Ion-ion streaming instability	Magnetosonic waves	$k \sim \frac{\omega_e}{c}$	$\gamma \sim \Omega_i$	Stabilized when the streaming velocity exceeds the Alfvén speed.
Kinetic cross-field streaming instability	Whistler mode waves with oblique propagation	$k \gtrsim \frac{\omega_{LH}}{V_0}$	$\omega \simeq \omega_{LH}$ $\gamma > \Omega_i$ $\omega \simeq \omega_{LH}$ $\gamma > \Omega_i$	The instability persists even if $V_0 \gg v_A$
Lower-hybrid-drift instability	Lower hybrid waves and drift waves	$k \sim \frac{\omega_{LH}}{V_0}$	$\omega \simeq \omega_{LH}$ $\gamma \gg \Omega_i$	Instability enhanced by ∇T_e
	Doppler-shifted whistler mode	$k > \frac{\omega_{LH}}{V_0}$	$\omega \simeq \omega_{LH}$ $\gamma \gg \Omega_i$	
Ion-acoustic instability	Ion waves	$k\lambda_D \lesssim 1$	$\omega \lesssim \omega_i$ $\gamma > \Omega_i$	Instability enhanced by ∇T_e
Electron-cyclotron drift instability	Doppler-shifted Bernstein waves and ion waves	$k\lambda_D \lesssim 1$	$\omega \simeq n\Omega_e$ $\gamma > \Omega_i$	Instability suppressed by ∇B
Whistler instability	Whistler-mode waves with parallel propagation	$k \lesssim \frac{\omega_e}{c}$	$\omega \ll \Omega_e$ $\gamma \gg \Omega_i$	

Wu+ 84

TABLE 1. Seven Instabilities Driven by Cross-Field Currents

Name	Type	Approximate Frequency	Wave Number of Growth Rate Maximum Growth Rate		Type of Resonance
Ion acoustic	e-s	$k(T_e/m_i)^{1/2}$	$k\lambda_{Debye} < 1$	$k_z \neq 0$	electron Landau
Buneman	e-s	$(m_e/m_i)^{1/3}\omega_{pe}$	$k \sim \omega_{pe}/v_d$	$k_z \neq 0$	nonresonant
Electron cyclotron drift	e-s	$k(T_e/m_i)^{1/2}$	$k\lambda_{Debye} < 1$	$k_z = 0$	electron cyclotron
Modified two-stream	e-s + e-m	Ω_{LH}	$ka_e < 1$	$k_z \neq 0$	nonresonant
Lower hybrid drift	e-s + e-m	Ω_{LH}	$ka_e \sim 1$	$k_z = 0$	nonresonant
Ion cyclotron drift	e-s + e-m	$n\Omega_i$*	$ka_e \sim 1$	$k_z = 0$	ion cyclotron
Ion drift ('universal')	e-s + e-m	$<<\Omega_i$	$ka_i \sim 1$	$k_z \neq 0$	electron Landau

The symbols used here are as defined in *Lemons and Gary* [1977]; e-s and e-m refer to electrostatic and electromagnetic, respectively.
*Parameter $n = 1, 2, 3, \cdots$.

Lemons&Gary 78

Vlasov equation

$$\frac{\partial f_s}{\partial t} + \boldsymbol{v} \cdot \nabla f_s + \frac{q_s}{m_s}\left(\boldsymbol{E} + \frac{\boldsymbol{v}}{c} \times \boldsymbol{B} \right) \cdot \nabla_u f_s = 0$$

configuration (3D) + velocity space (3D) = 6D

Vlasov simulation (Euler)

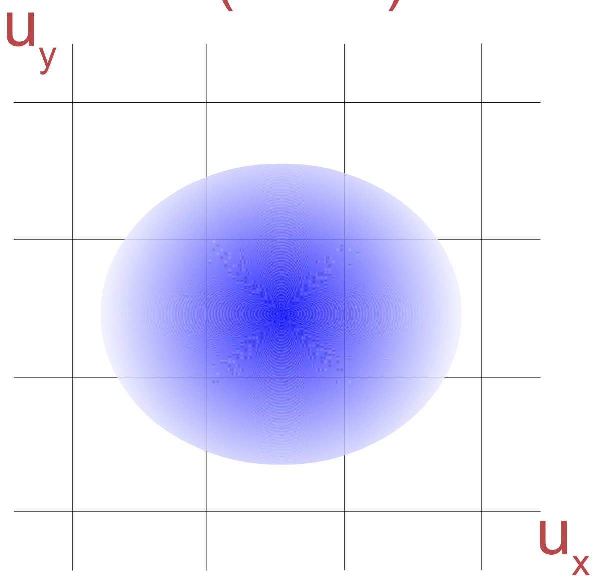

Particle-in-Cell simulation (Lagrangian)

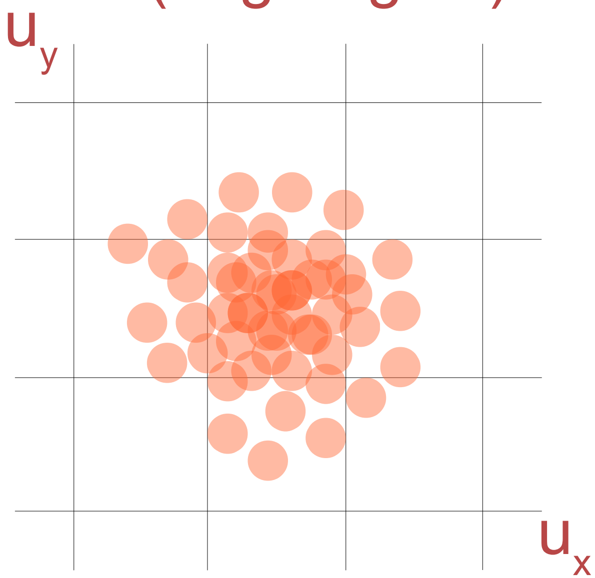

Maxwell equation

$$\frac{\partial \boldsymbol{B}}{\partial t} = -c \nabla \times \boldsymbol{E}$$

$$\frac{\partial \boldsymbol{E}}{\partial t} = c \nabla \times \boldsymbol{B} - 4\pi \boldsymbol{J}$$

with $\nabla \cdot \boldsymbol{B} = 0$
$\nabla \cdot \boldsymbol{E} = 4\pi \rho_e$

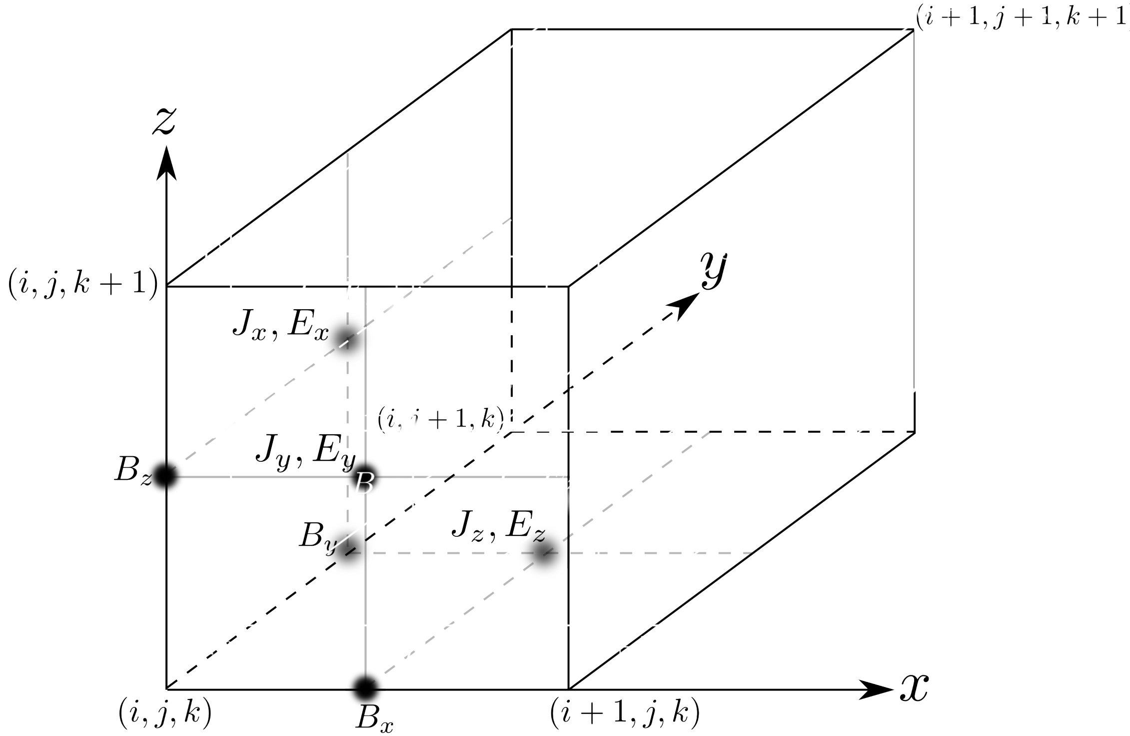

Implicit FDTD method

$$\left(I - (\theta c \Delta t)^2 \nabla^2\right) \delta \boldsymbol{B} = \theta (c \Delta)^2 \left(\nabla^2 \boldsymbol{B}^t + \frac{4\pi}{c} \nabla \times J^{t+\Delta t/2} \right) - c \Delta t \nabla \times \boldsymbol{E}^t$$

θ : implicitness factor

solved within ~10 interations by the conjugate gradient method

Particle-in-Cell simulation

Particle push

$$\frac{d\boldsymbol{x}_p}{dt} = \frac{\boldsymbol{u}_p}{\gamma_p}$$

$$\frac{d\boldsymbol{u}_p}{dt} = \frac{q}{m}\left(\boldsymbol{E} + \frac{\boldsymbol{u}_p}{c\gamma_p} \times \boldsymbol{B}\right)$$

$$\boldsymbol{J} = \sum_p q_p \frac{\boldsymbol{u}_p}{\gamma_p}$$

Maxwell equation

$$\frac{\partial \boldsymbol{B}}{\partial t} = -c\nabla \times \boldsymbol{E}$$

$$\frac{\partial \boldsymbol{E}}{\partial t} = c\nabla \times \boldsymbol{B} - 4\pi \boldsymbol{J}$$

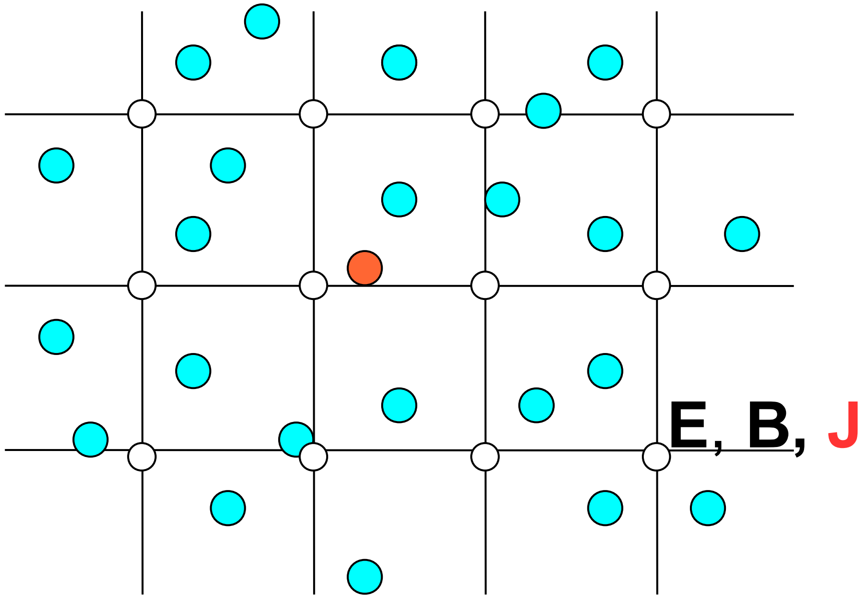

Particle-in-Cell simulation

Particle push

$$\frac{d\boldsymbol{x}_p}{dt} = \frac{\boldsymbol{u}_p}{\gamma_p}$$

$$\frac{d\boldsymbol{u}_p}{dt} = \frac{q}{m}\left(\boldsymbol{E} + \frac{\boldsymbol{u}_p}{c\gamma_p} \times \boldsymbol{B}\right)$$

$$\boldsymbol{J} = \sum_p q_p \frac{\boldsymbol{u}_p}{\gamma_p}$$

Maxwell equation

$$\frac{\partial \boldsymbol{B}}{\partial t} = -c\nabla \times \boldsymbol{E}$$

$$\frac{\partial \boldsymbol{E}}{\partial t} = c\nabla \times \boldsymbol{B} - 4\pi \boldsymbol{J}$$

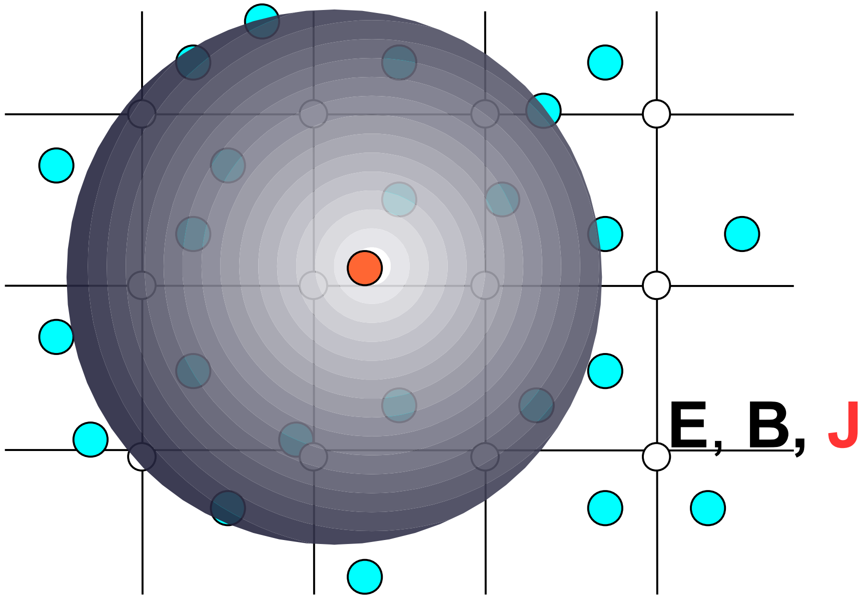

Characteristic scales in PIC simulations

- $\Delta h \sim$ Debyle length λ_D:

$$\lambda_D[m] = 7.4\, T^{\frac{1}{2}}[eV] \left(\frac{1}{n[cm^{-3}]} \right)^{\frac{1}{2}}$$

- $\Delta t \sim$ electron plasma frequency ω_{pe}^{-1}:

$$\omega_{pe}^{-1}[sec] = \frac{1}{9} \left(\frac{1}{n[cm^{-3}]} \right)^{\frac{1}{2}} 10^{-3}$$

- Proton-to-Electron mass ratio M/m:

$M/m \sim O(10)$ ($\leftrightarrow$ 1836)

parsec and $10^{3\text{-}6}$ yrs in astrophysics!

Characteristic scales of SNR shocks

- Shock speed
  - V_{sh} = 1000 – 10000 km/s
  - non-relativistic shocks

- Magnetic field (upstream)
  - a few μG : Alfven speed V_A ~ 10 km/s (n~0.1 /cc)
  - (Alfven) Mach number M > 100 !

- Dynamic ranges
  - shock scale : MHD ($L \gg r_{gi} \gg r_{ge}$)
  - Ion to Electron mass ratio M/m=1836
  - relativistic electrons : v~c ($\gg V_{sh} > V_A$)

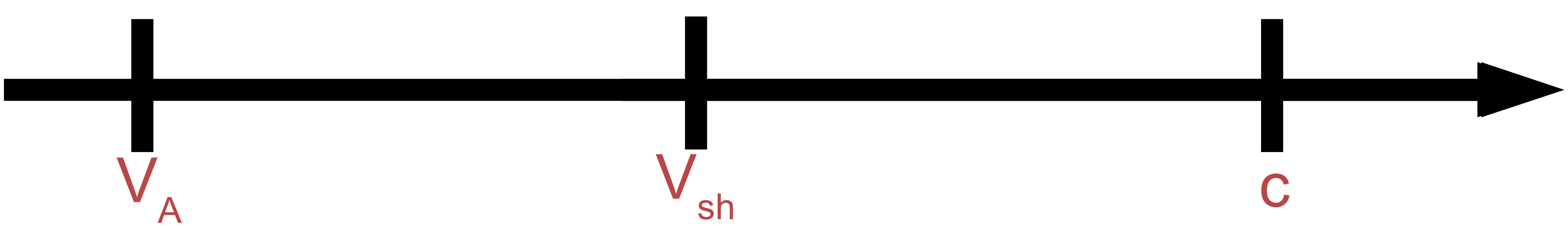

In-house PIC code

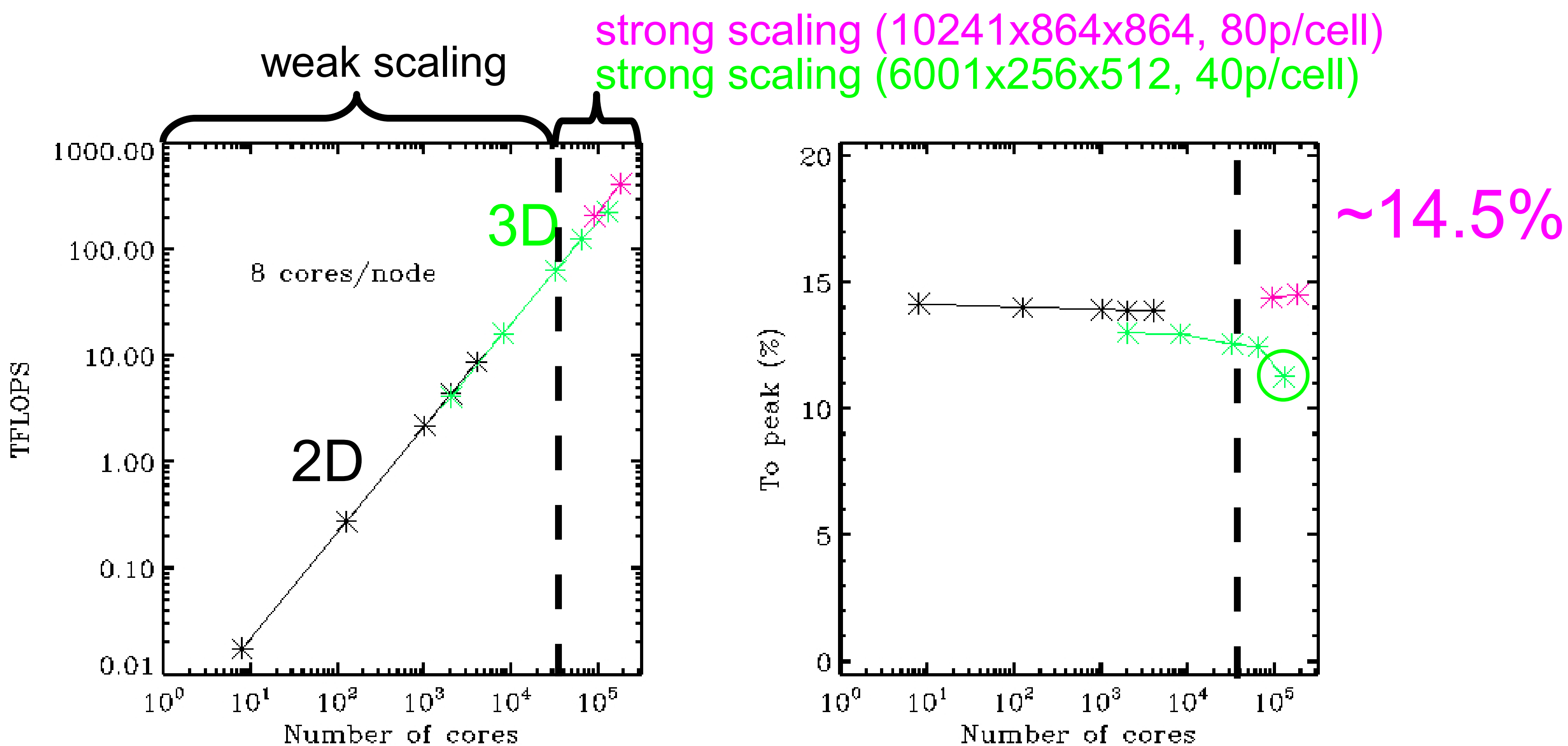

- Optimized on K computer at AICS, RIKEN
- Fully SIMD optimized (vectorized)
- MPI+OpenMP hybrid parallelization
- Implicit FDTD
- High-accuracy current deposit algorithm (Esirkepov '01)
- Quadratic spline for shape function

Shock creation - Injection method

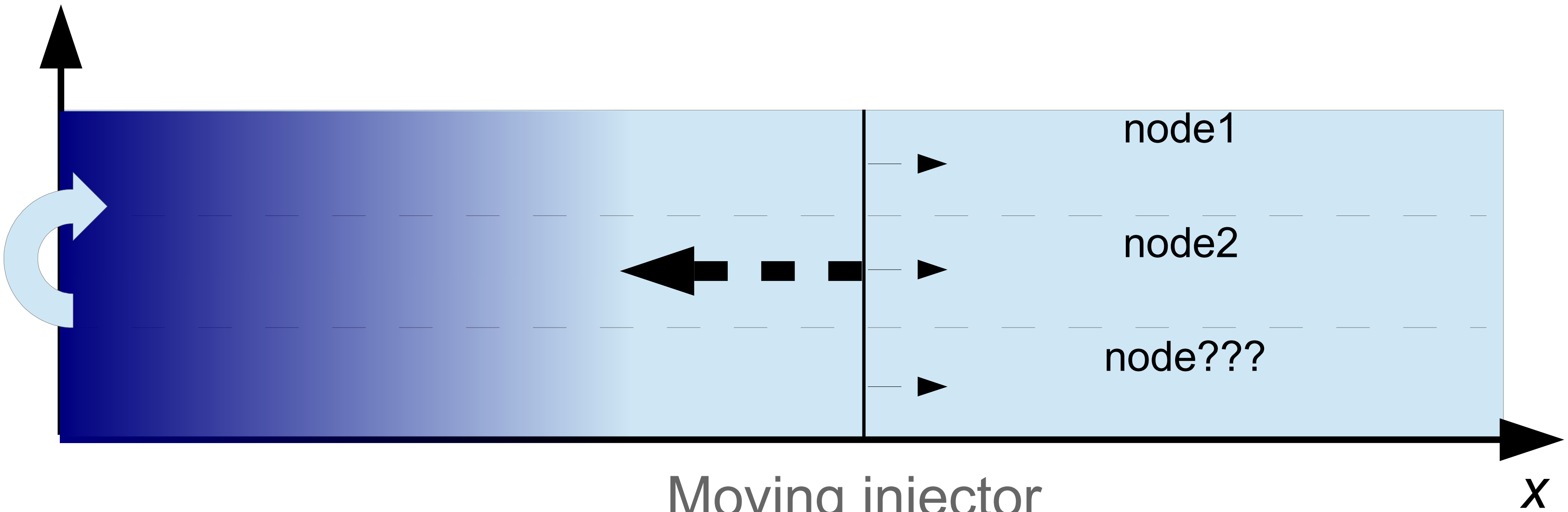

Moving injector
(Riquelme & Spitkovsky '11)

Physics in high M_A shocks

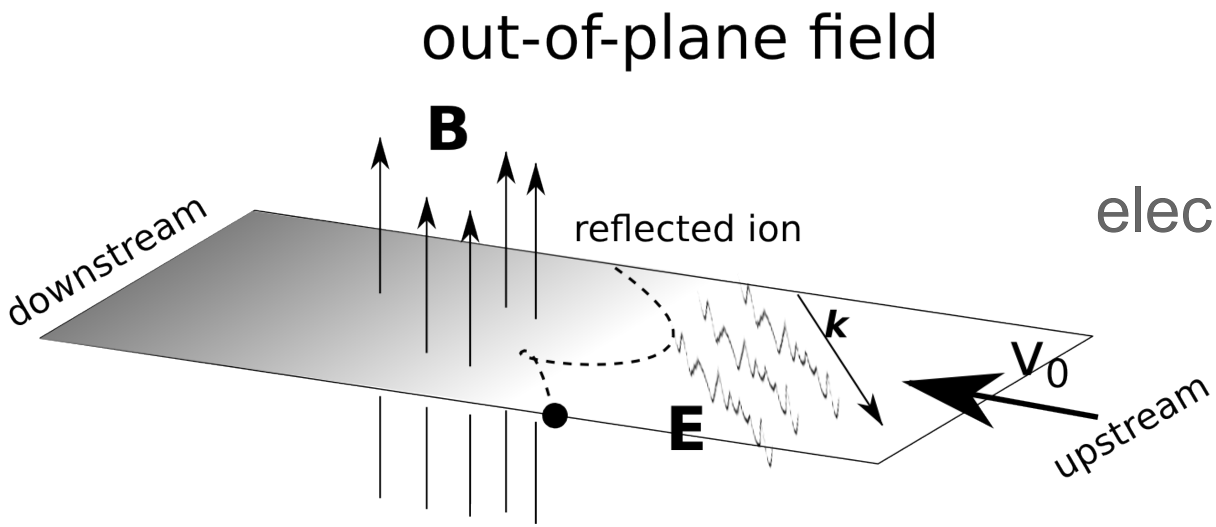

k **perp** $\mathbf{B_0}$

elecron pre-acceleration

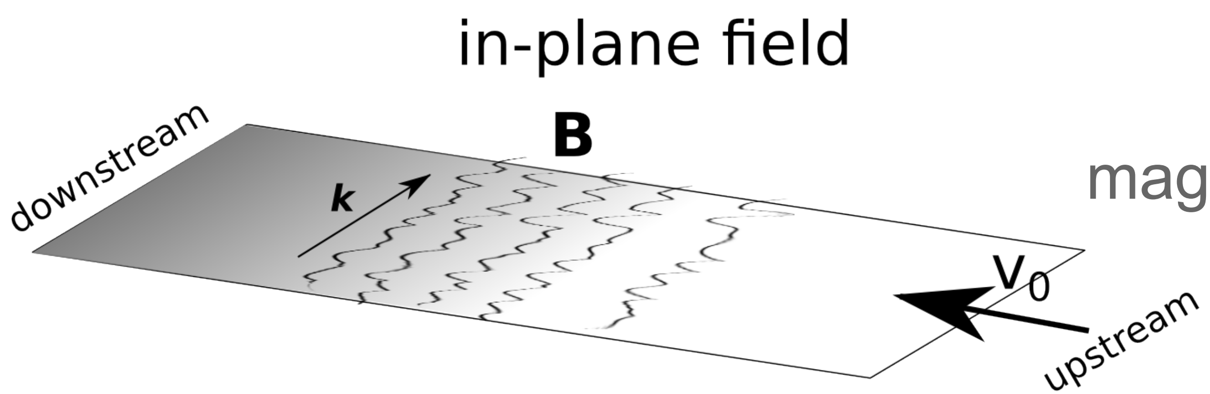

k **//** $\mathbf{B_0}$

magnetic field turbulence

Physics in high M_A shocks

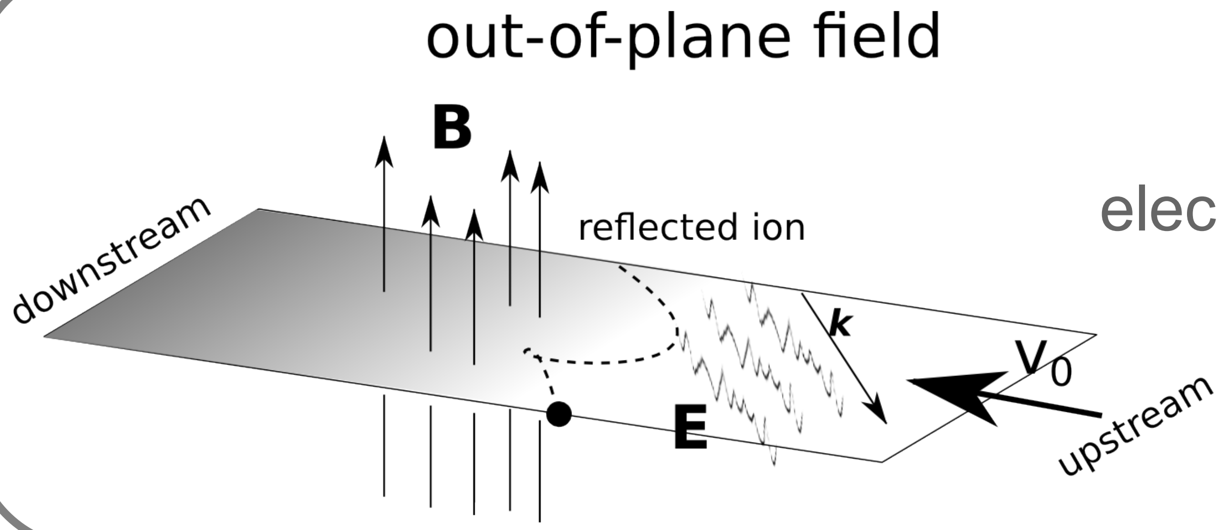

k perp $\mathbf{B}_0$
elecron pre-acceleration

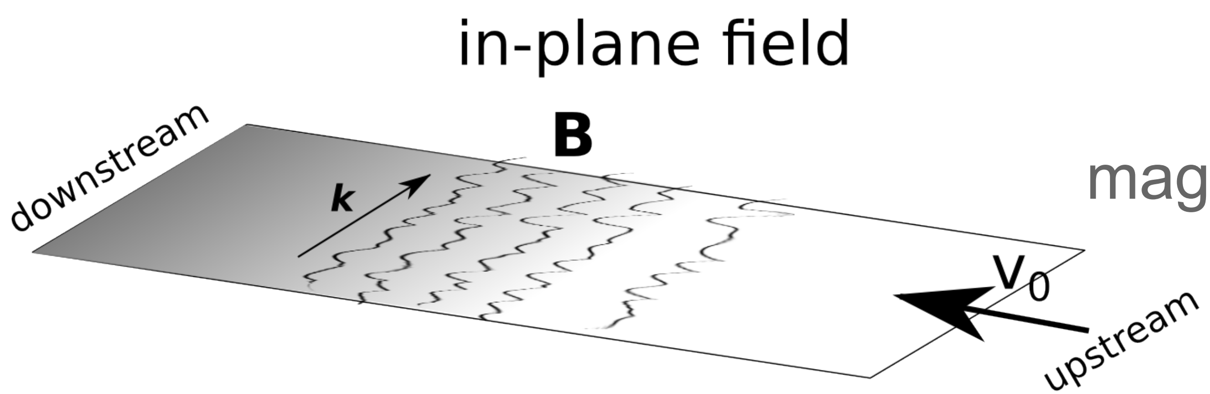

k // $\mathbf{B}_0$
magnetic field turbulence

Electron shock surfing acceleration (eSSA)

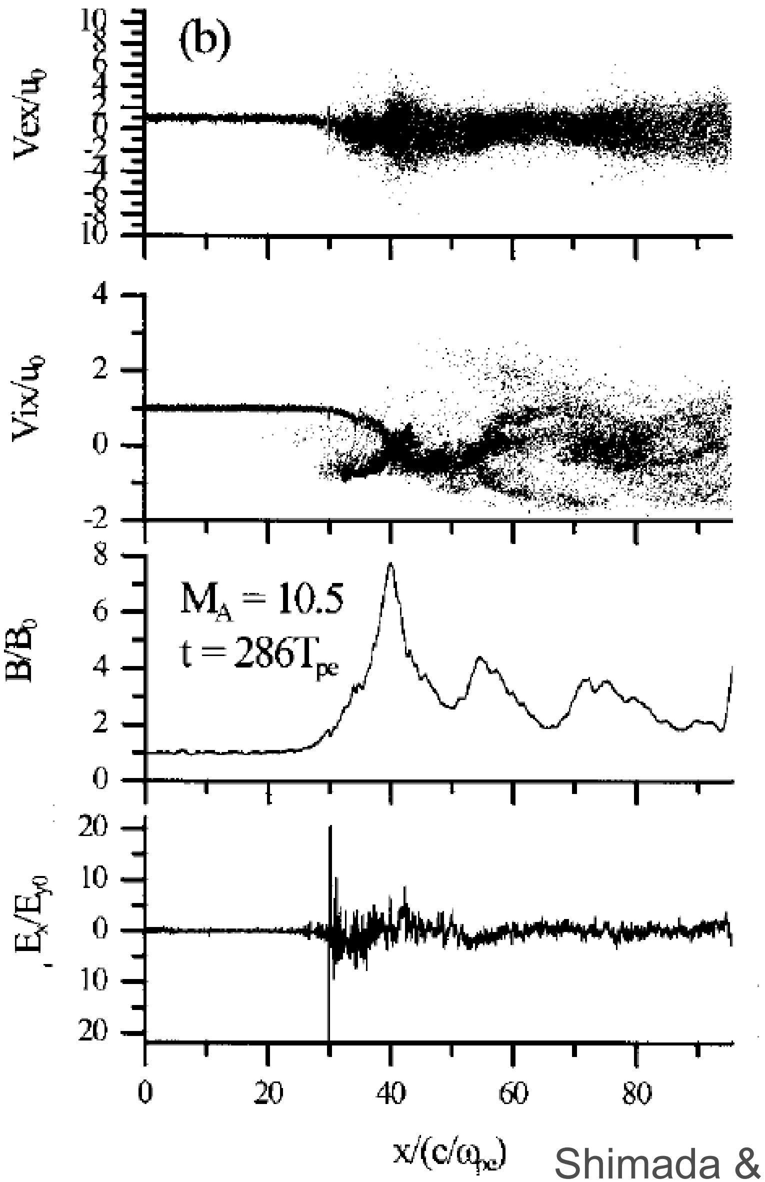

Shimada & Hoshino '00

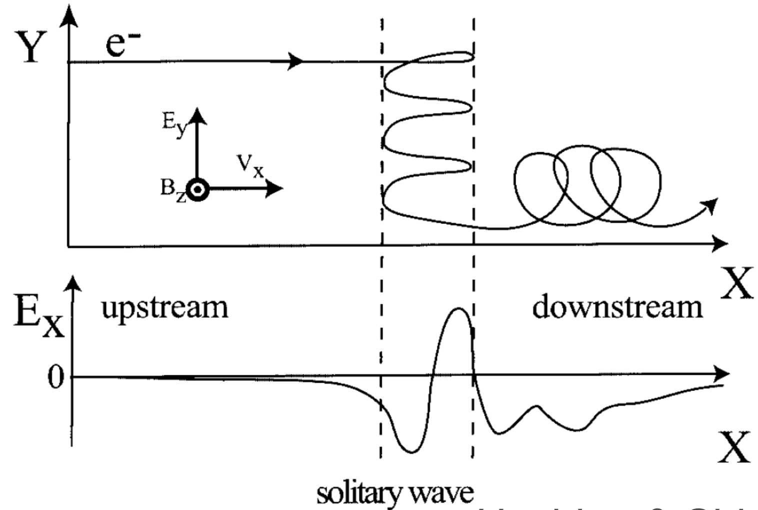

Hoshino & Shimada '02

Linear unstable condition

$$M_A > \sqrt{\frac{M}{m}}\sqrt{\beta_e}$$

Trapping condition

$$M_A > \left(\frac{M}{m}\right)^{2/3}$$

Matsumoto+ '12

eSSA in multi dimensions ?

M/m=25, M_A~15

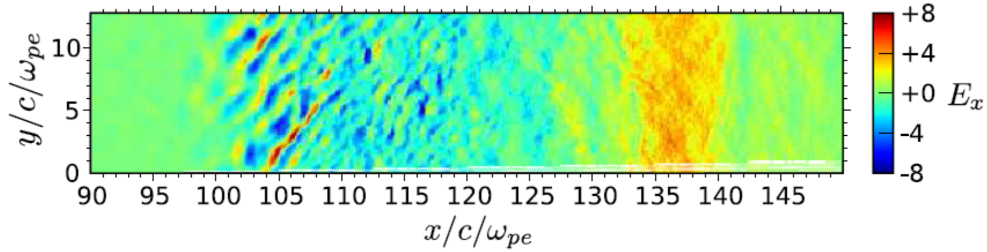

Amano & Hoshino '09

multi-dimensinonal effects

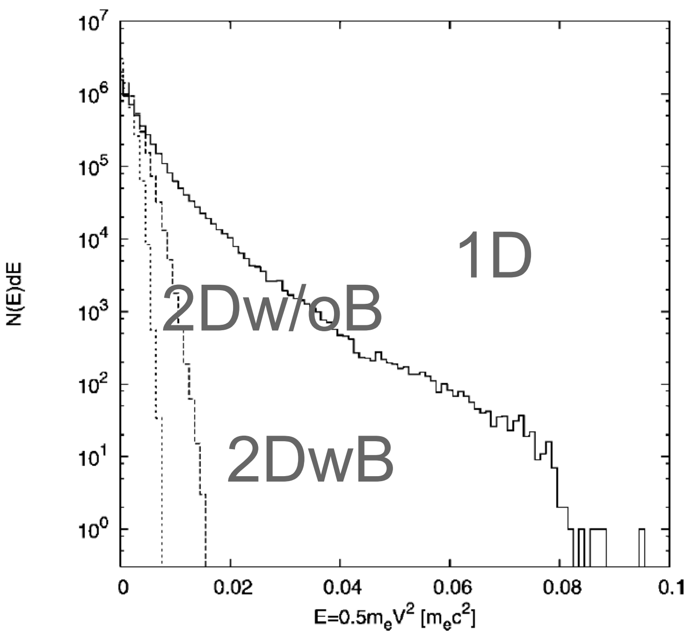

Ohira & Takahara '07

*periodic system modeling foot region

mass ratio dependence
(M/m=25, 100, 400)

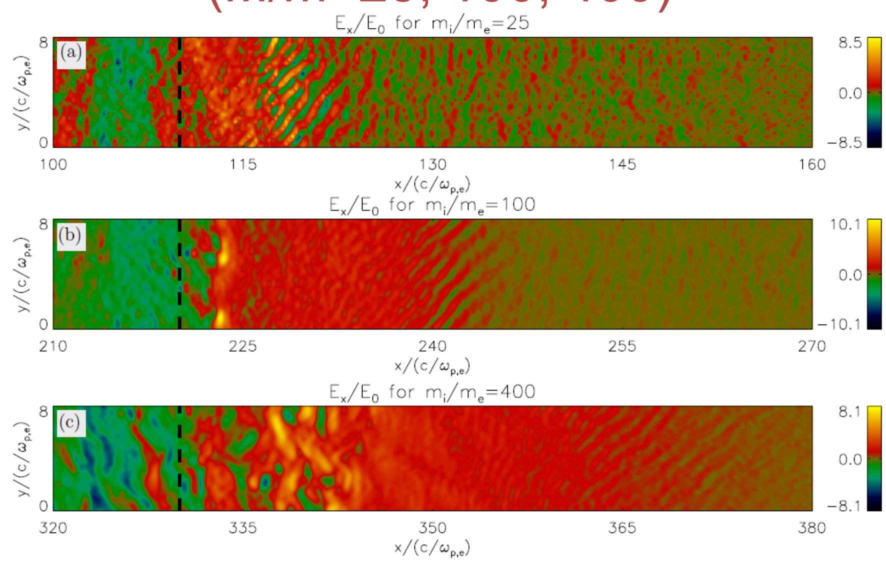

Riquelme & Spitkovsky '11

2D PIC simulations of perpendicular shocks

Trapping condition

Linear unstable condition

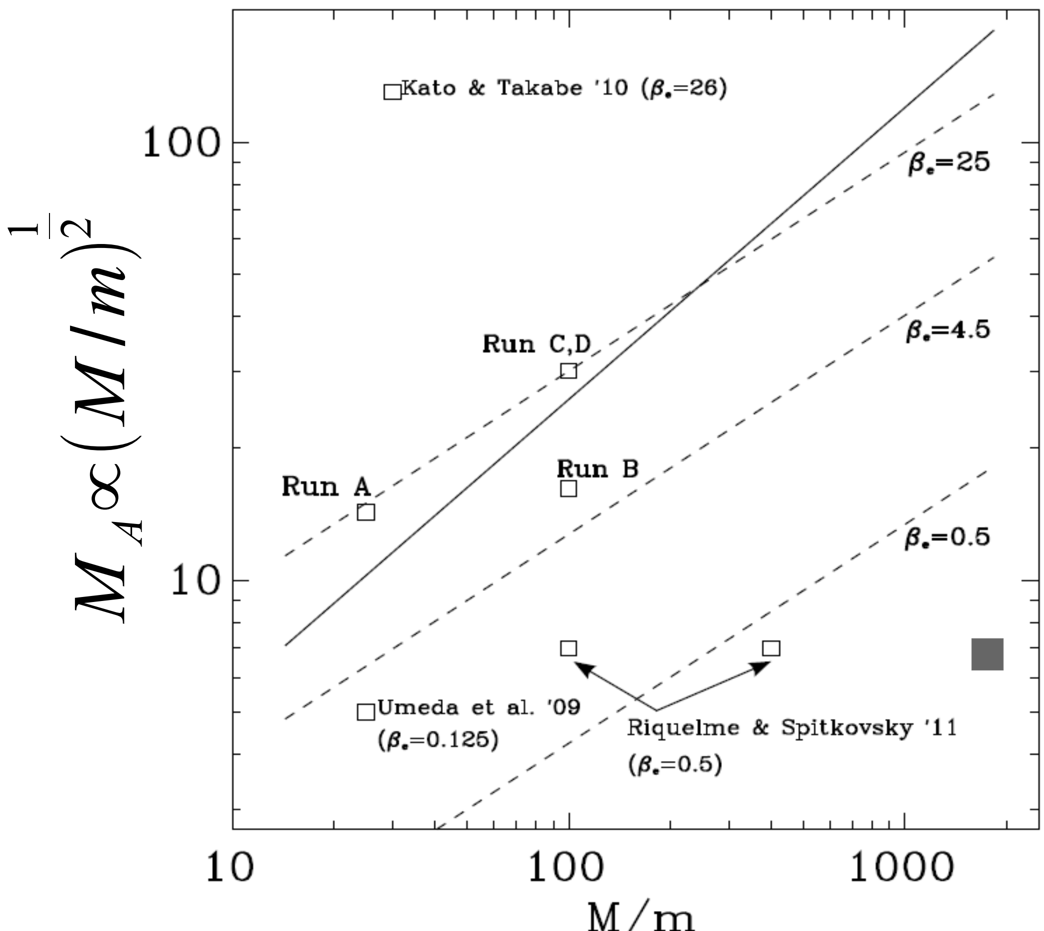

Matsukiyo & YM

Matsumoto+ '12

2D PIC simulations of perpendicular shocks

Trapping condition

Linear unstable condition

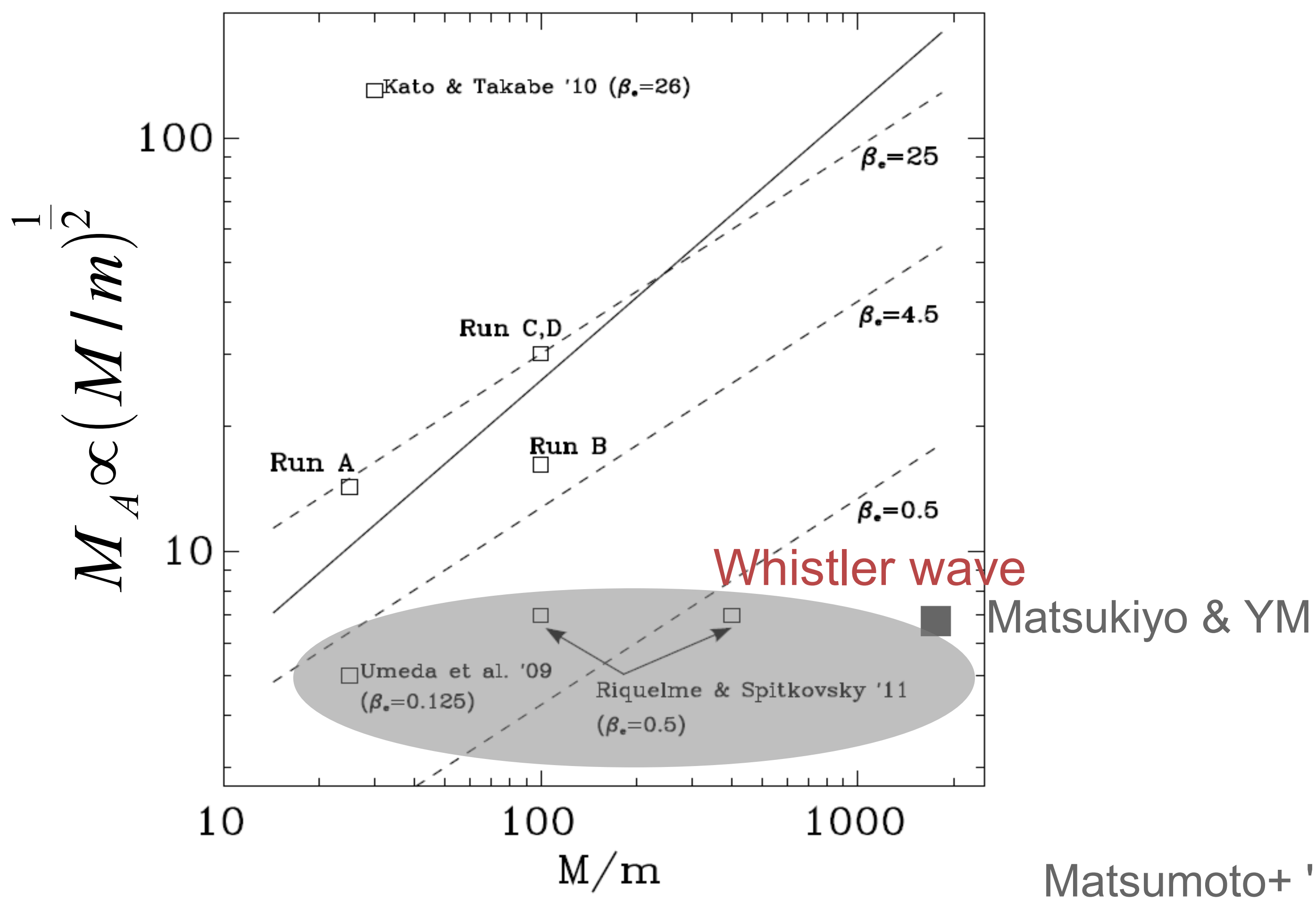

Matsumoto+ '12

2D PIC simulations of perpendicular shocks

Trapping condition — Linear unstable condition

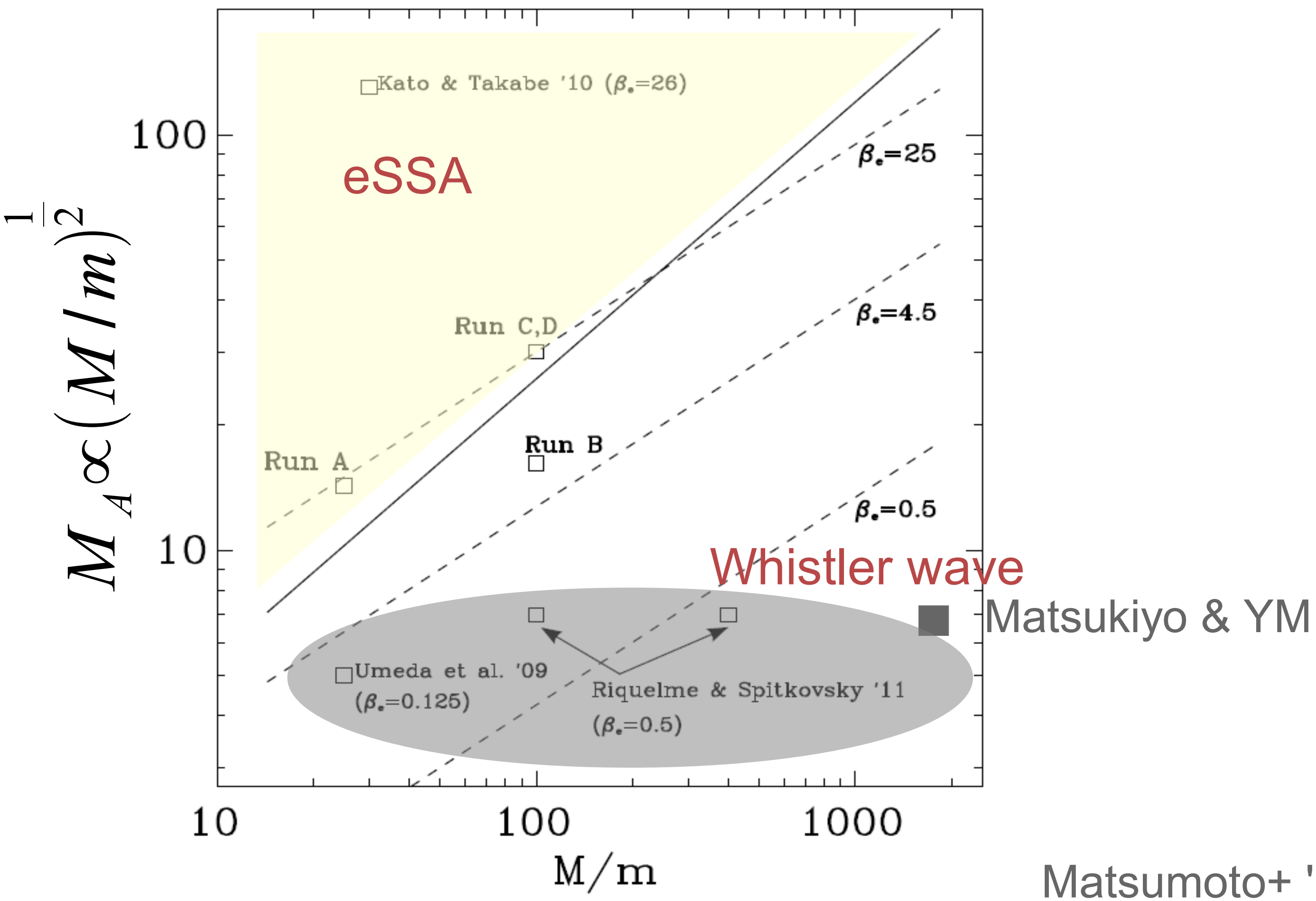

Matsumoto+ '12

2D PIC simulations of perpendicular shocks

Trapping condition (solid line) Linear unstable condition (dashed line)

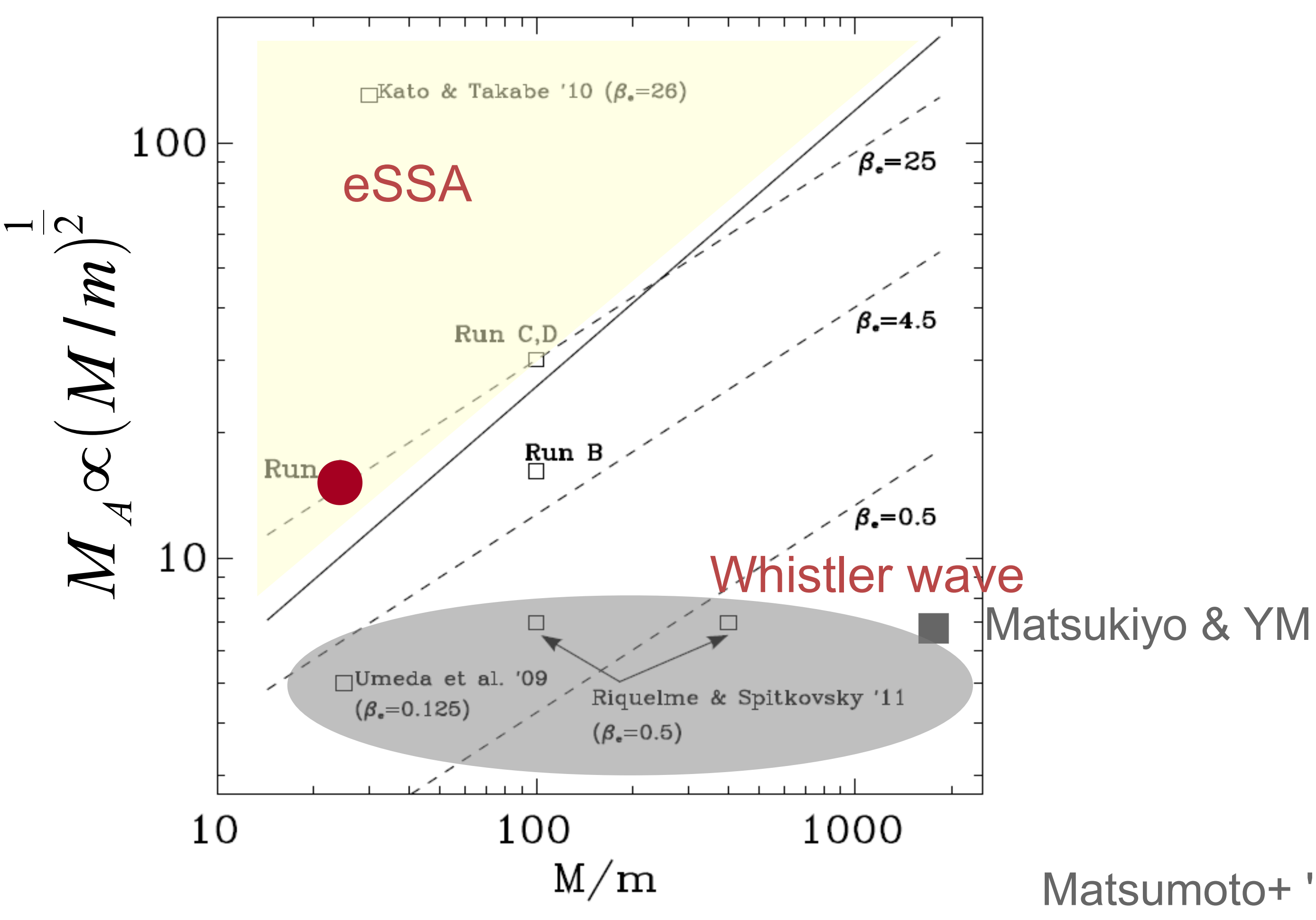

Matsumoto+ '12

2D PIC simulations of perpendicular shocks

Trapping condition

Linear unstable condition

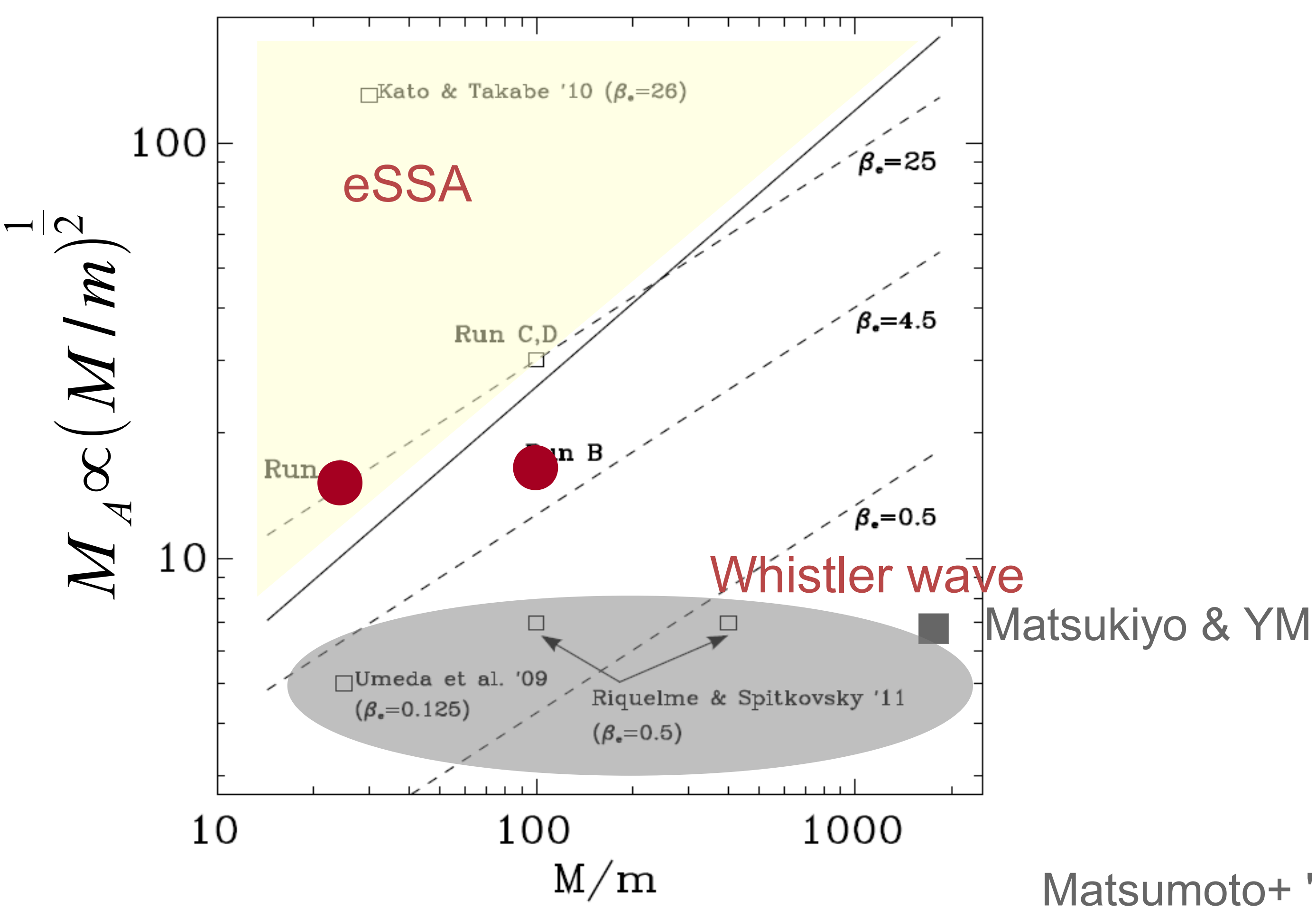

Matsumoto+ '12

2D PIC simulations of perpendicular shocks

Trapping condition

Linear unstable condition

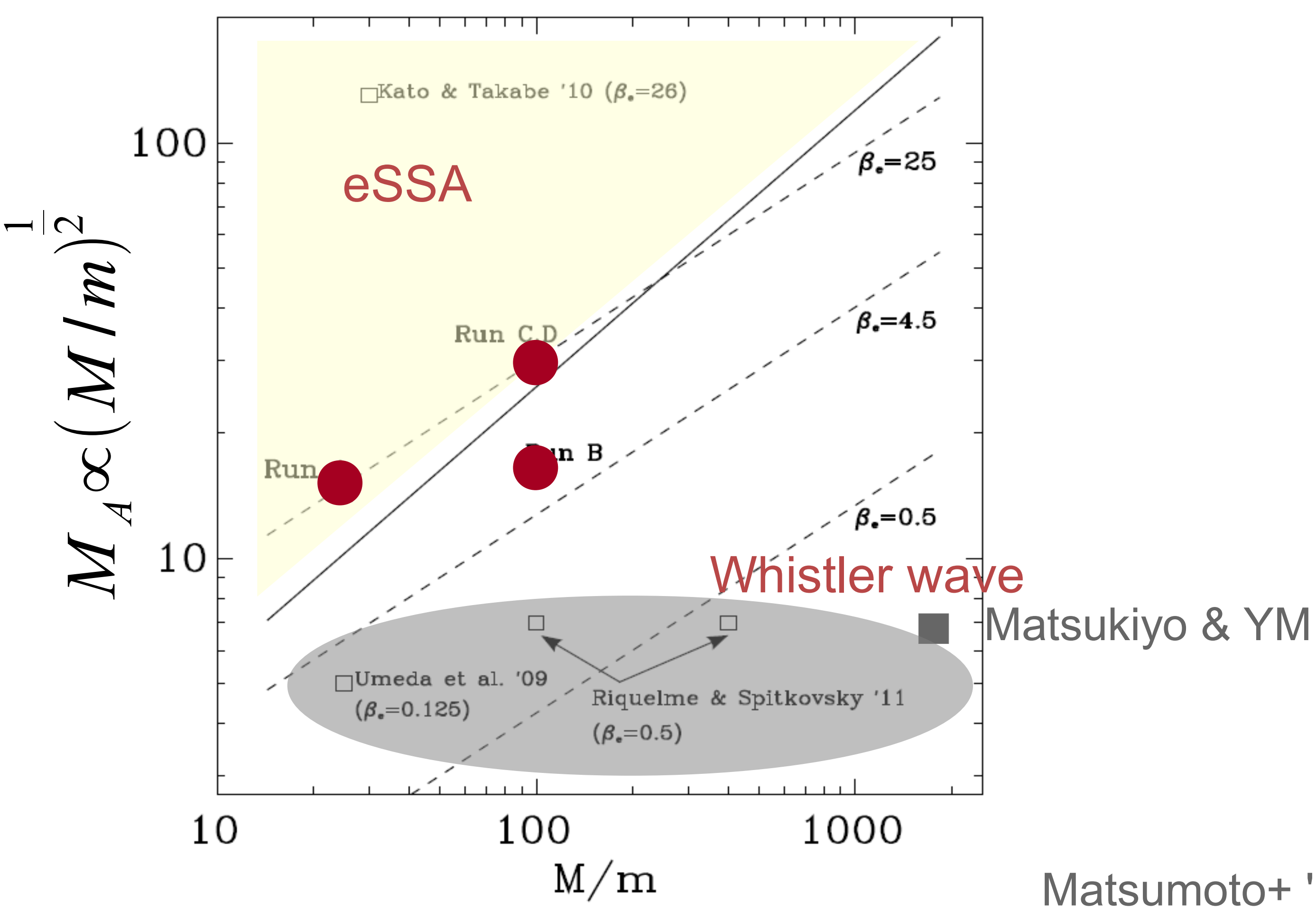

Matsumoto+ '12

2D PIC simulations of perpendicular shocks

Trapping condition

Linear unstable condition

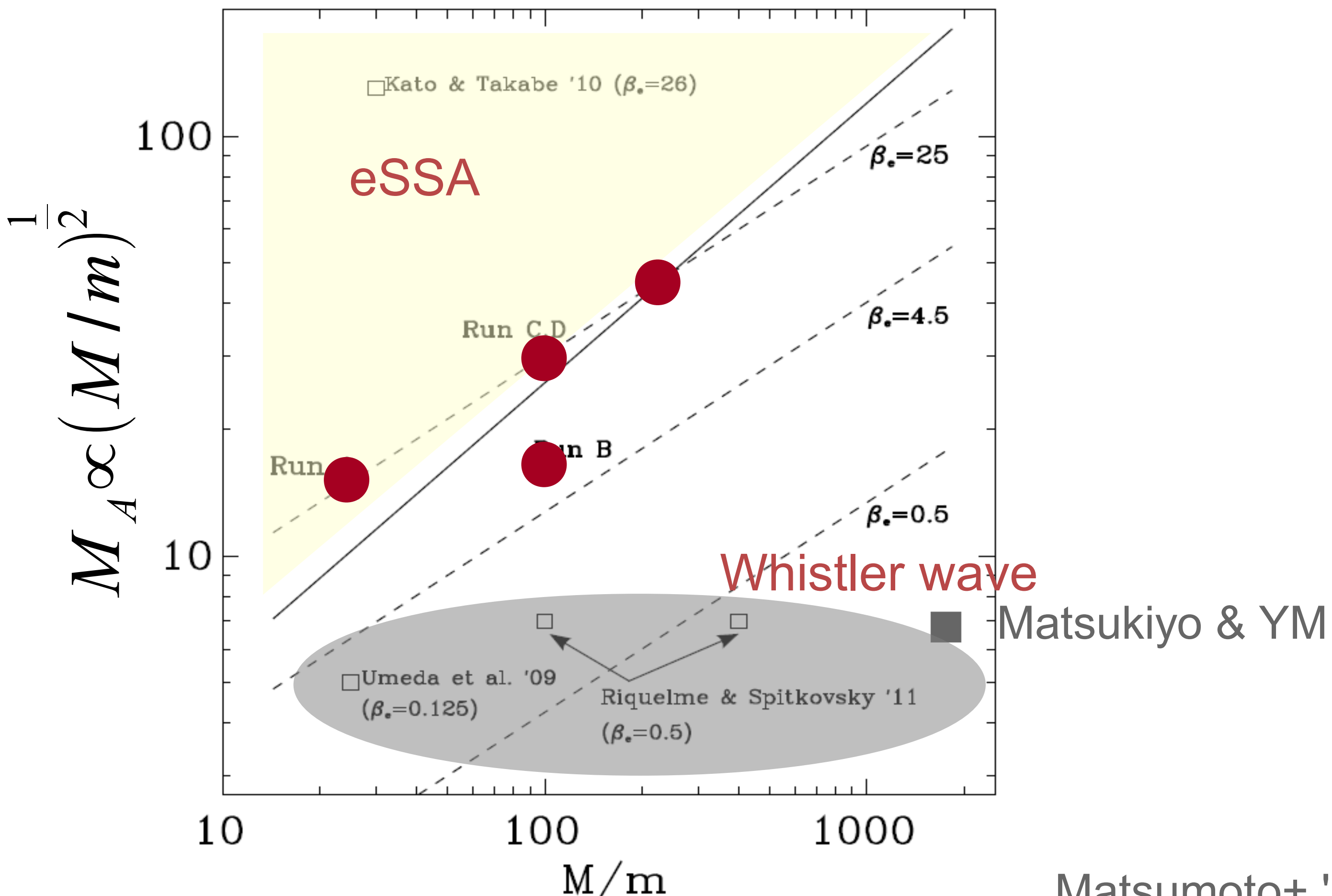

Matsumoto+ '12

e- acceleration at M/m=225, M_A~45 shock

$|E_{es}|/B_0$

downstream

upstream

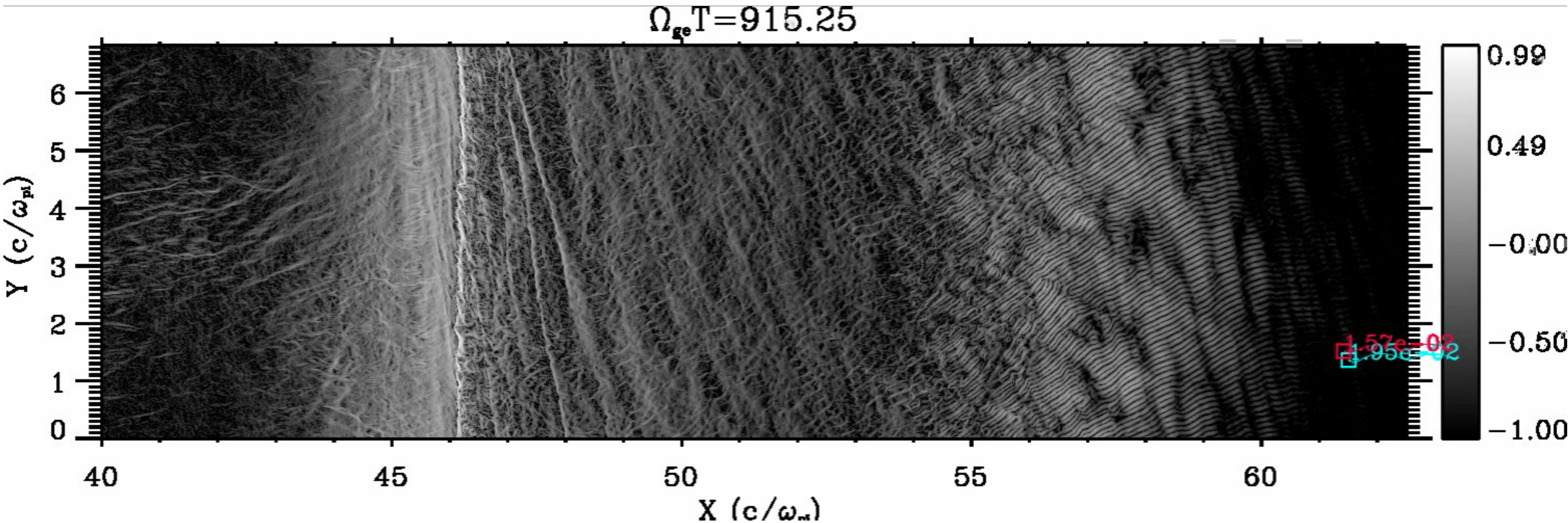

Matsumoto+ '13 *PRL*

:accelerated

:thermal

Overview ($\Omega_{gi}T$~4)

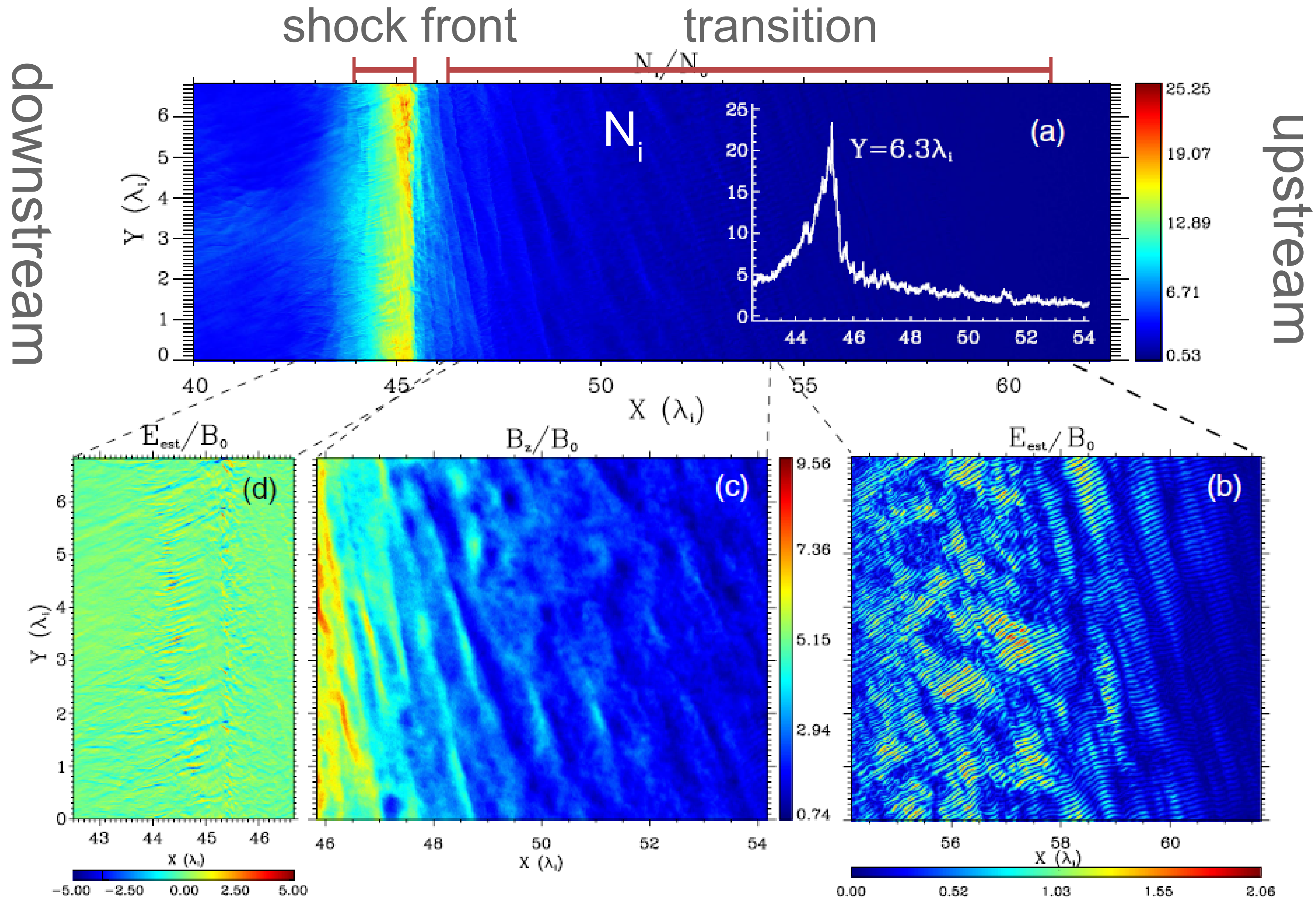

Various kinetic instabilities

- Leading edge
  - strong Buneman instability
  - efficient electron acceleration
- Transition region
  - ion-beam Weibel instability (Kato & Takabe '11)
  - self-generated current sheets
- Shock front
  - strong electrostatic field
  - Ion acoustic instability (by pre-heated electron + 2 ion components)

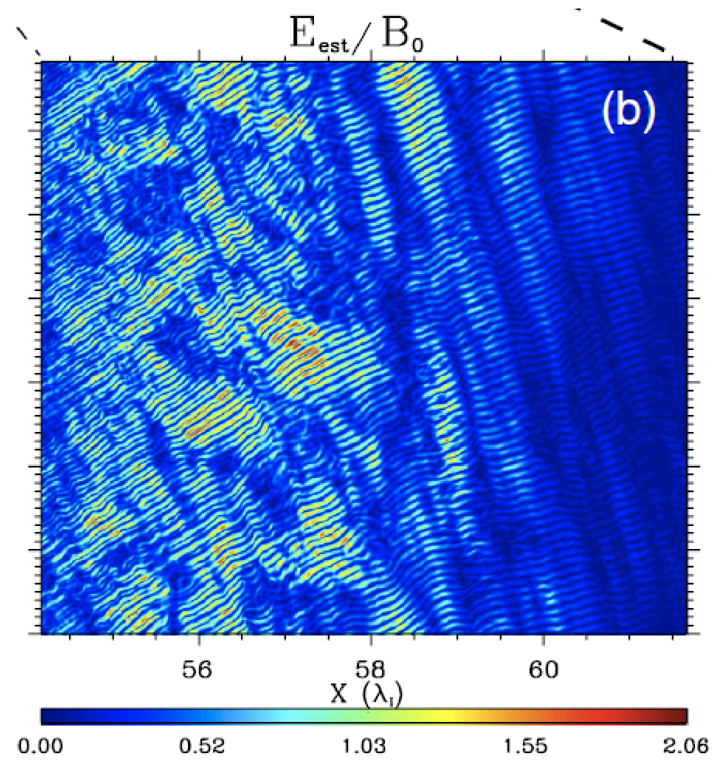

Various kinetic instabilities

- Leading edge
  - strong Buneman instability
  - efficient electron acceleration
- Transition region
  - ion-beam Weibel instability (Kato & Takabe '11)
  - self-generated current sheets
- Shock front
  - strong electrostatic field
  - Ion acoustic instability (by pre-heated electron + 2 ion components)

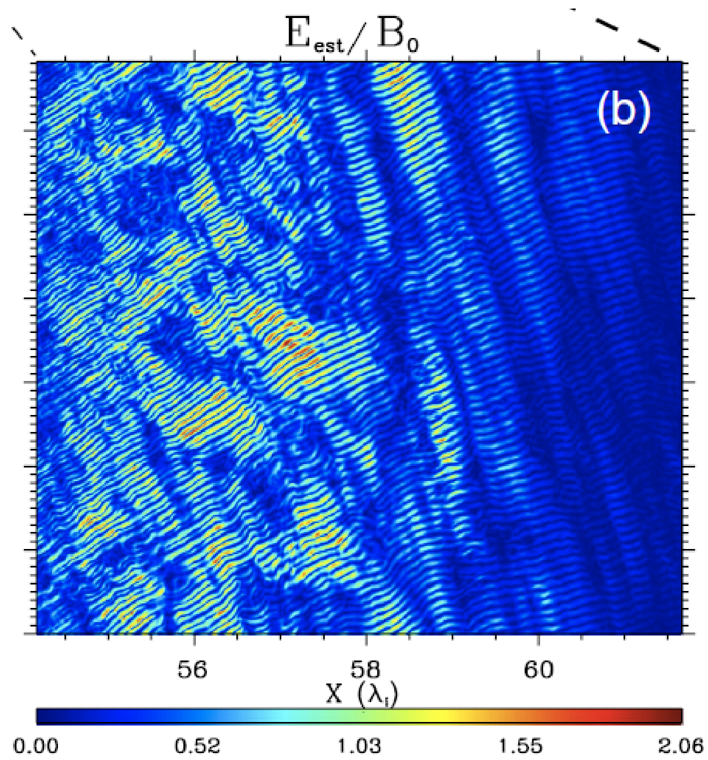

Various kinetic instabilities

- Leading edge
  - strong Buneman instability
  - efficient electron acceleration
- Transition region
  - ion-beam Weibel instability (Kato & Takabe '11)
  - self-generated current sheets
- Shock front
  - strong electrostatic field
  - Ion acoustic instability (by pre-heated electron + 2 ion components)

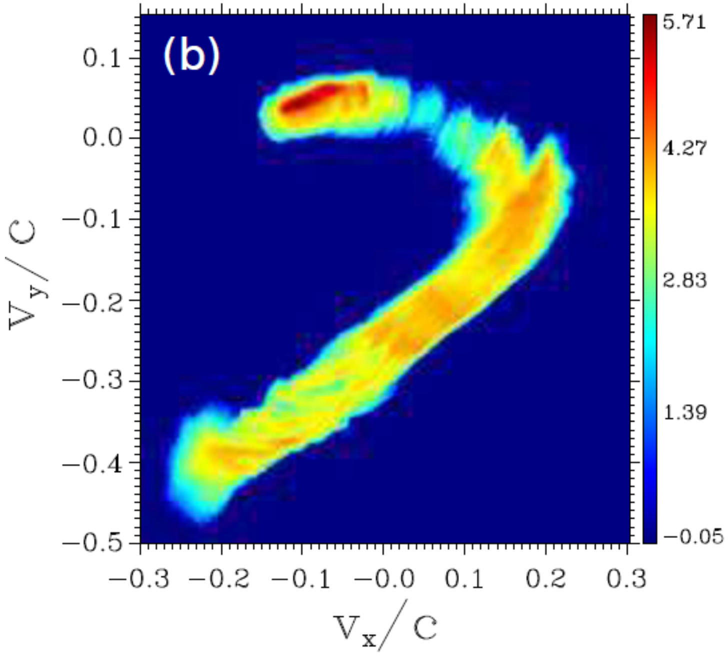

Various kinetic instabilities

- Leading edge
  - strong Buneman instability
  - efficient electron acceleration
- Transition region
  - ion-beam Weibel instability (Kato & Takabe '11)
  - self-generated current sheets
- Shock front
  - strong electrostatic field
  - Ion acoustic instability (by pre-heated electron + 2 ion components)

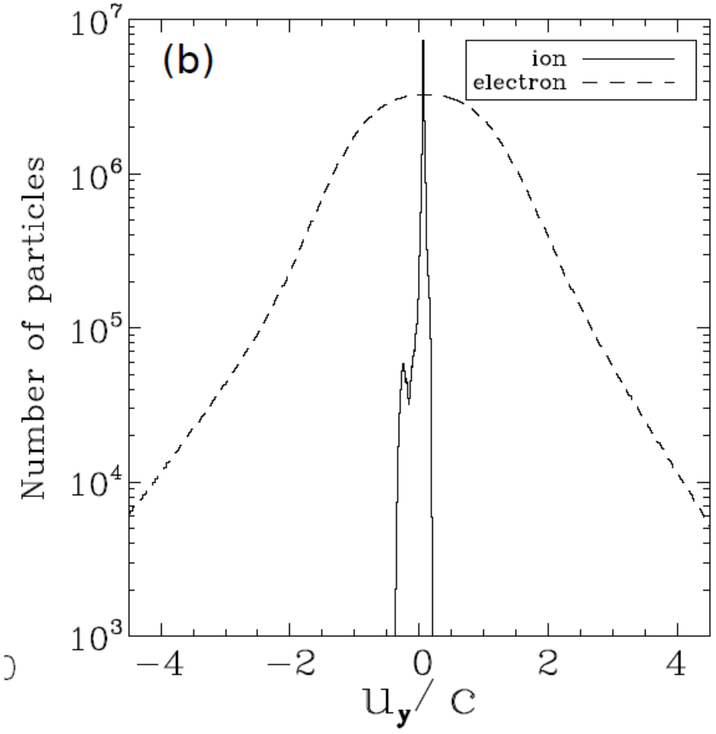

Electron downstream energy spectra

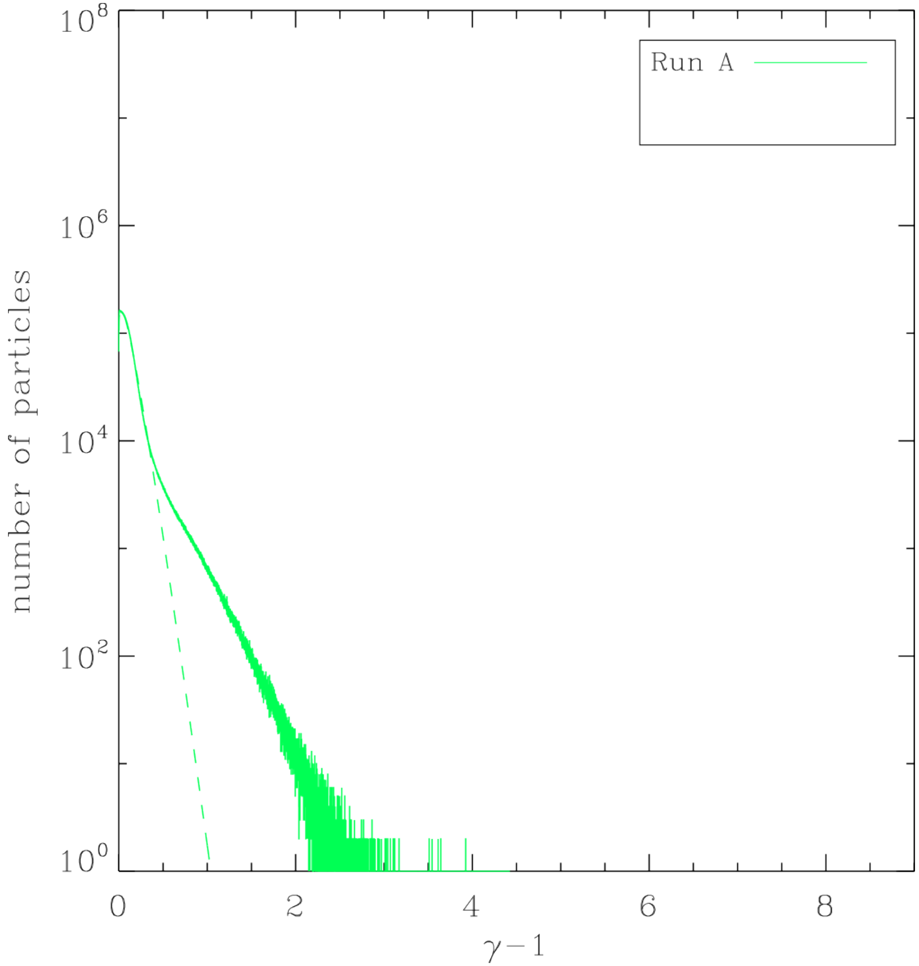

SNR shocks

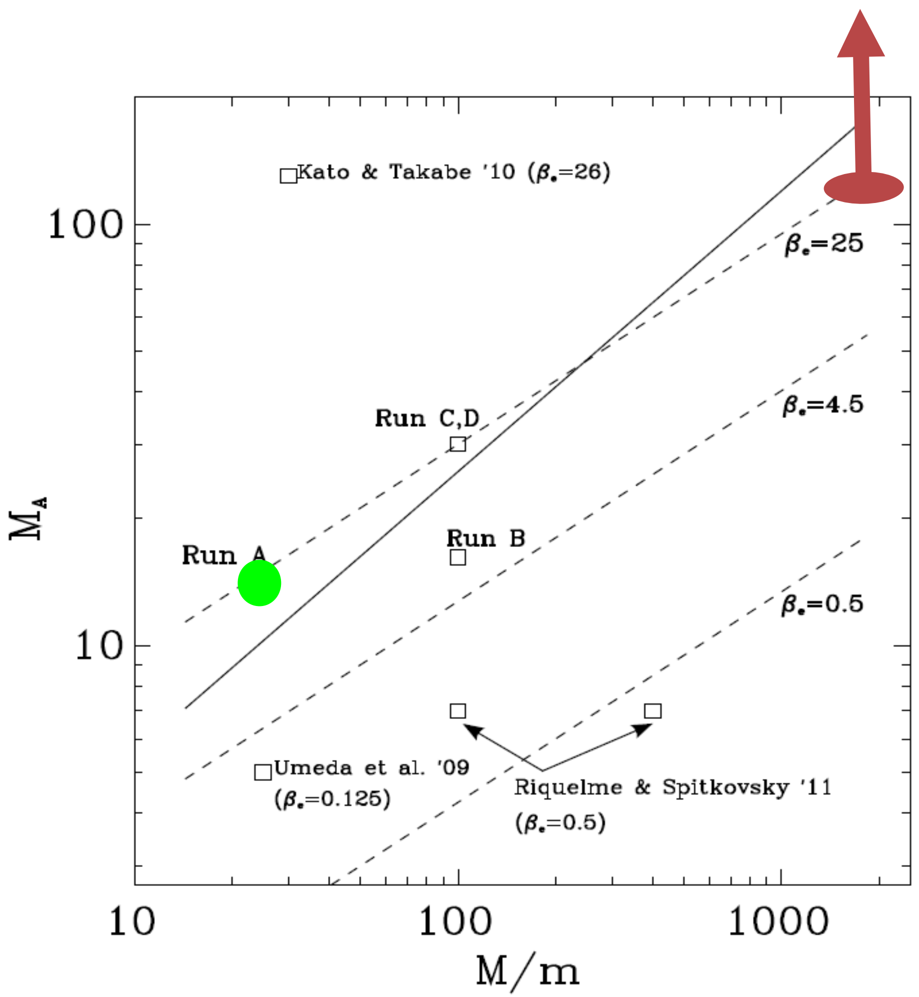

Matsumoto+ '12, '13

Electron downstream energy spectra

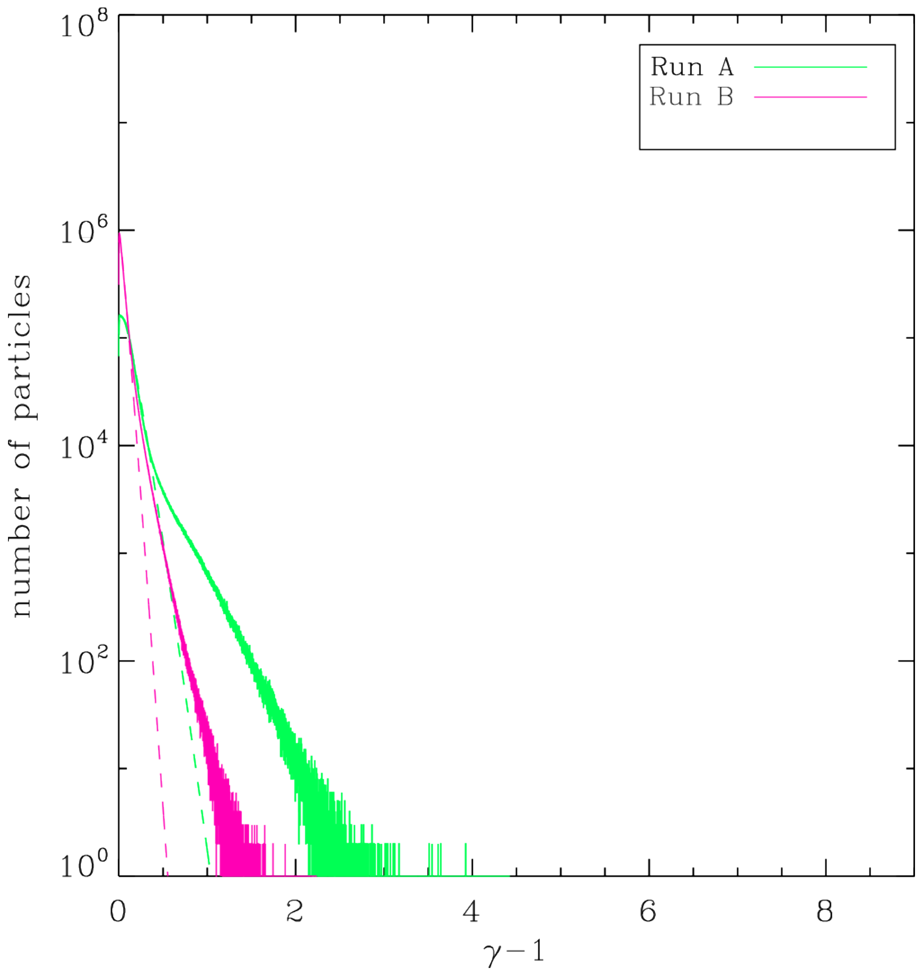

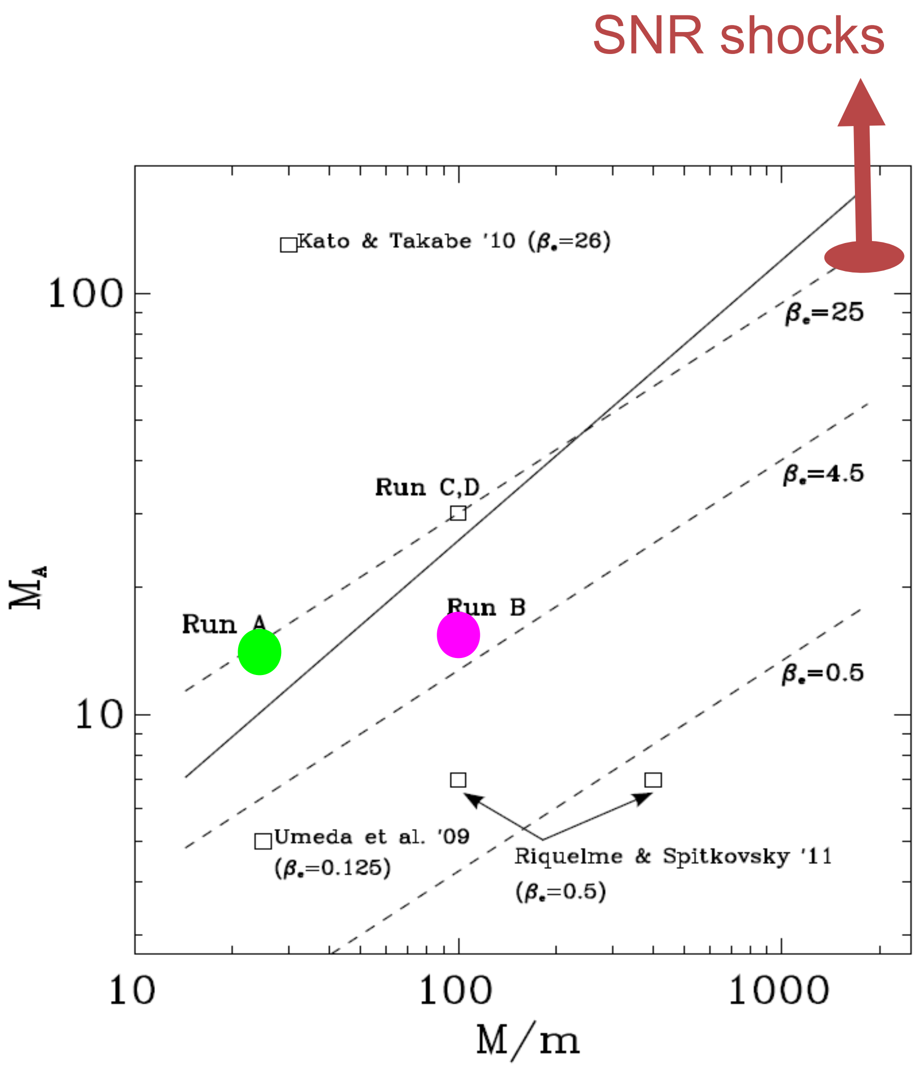

Matsumoto+ '12, '13

Electron downstream energy spectra

SNR shocks

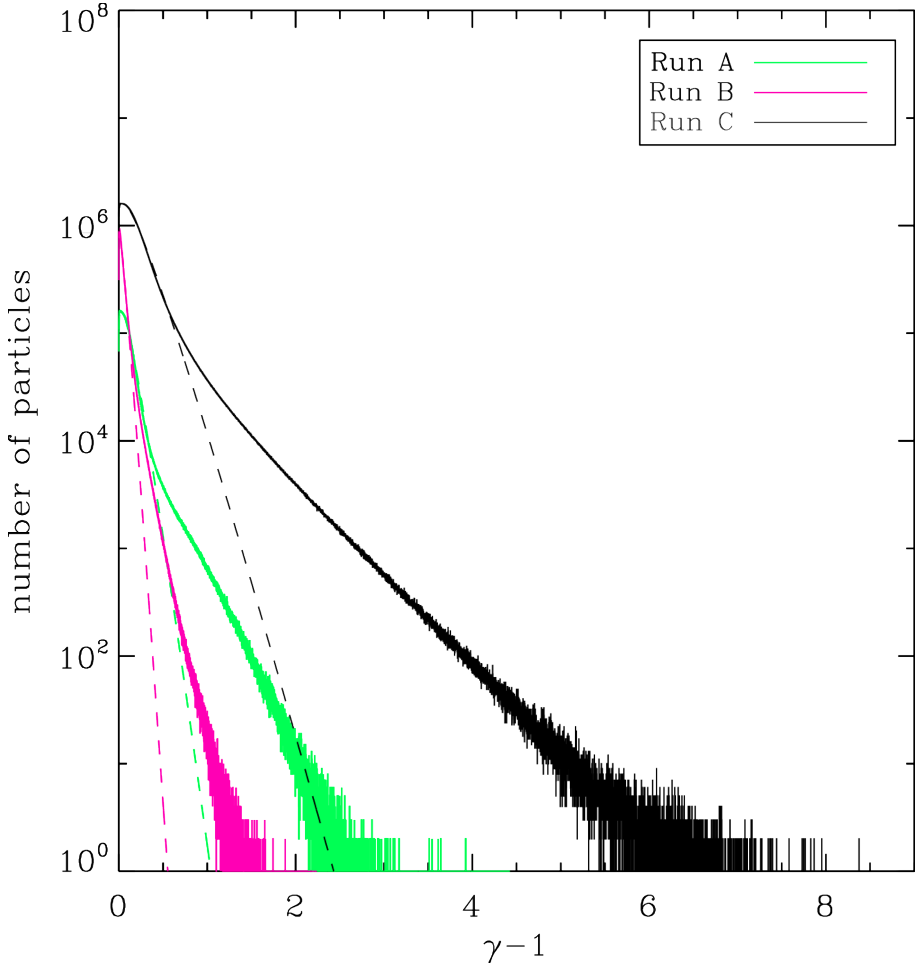

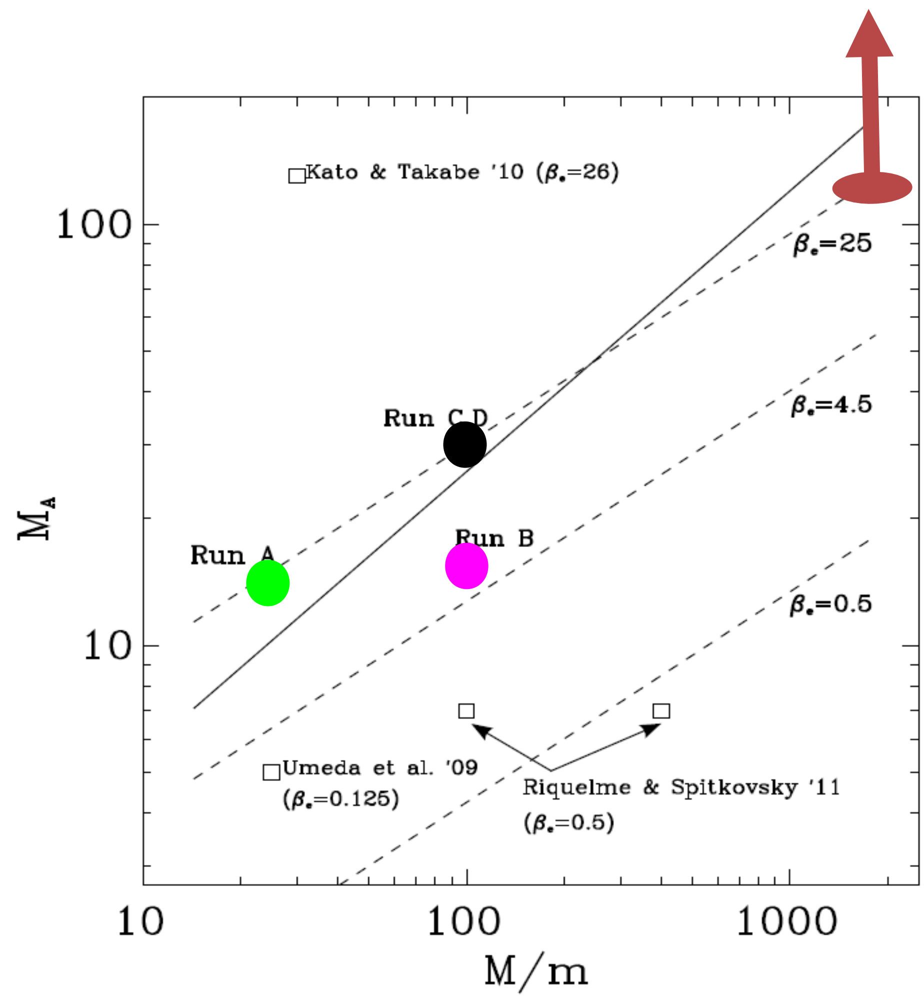

Matsumoto+ '12, '13

Electron downstream energy spectra

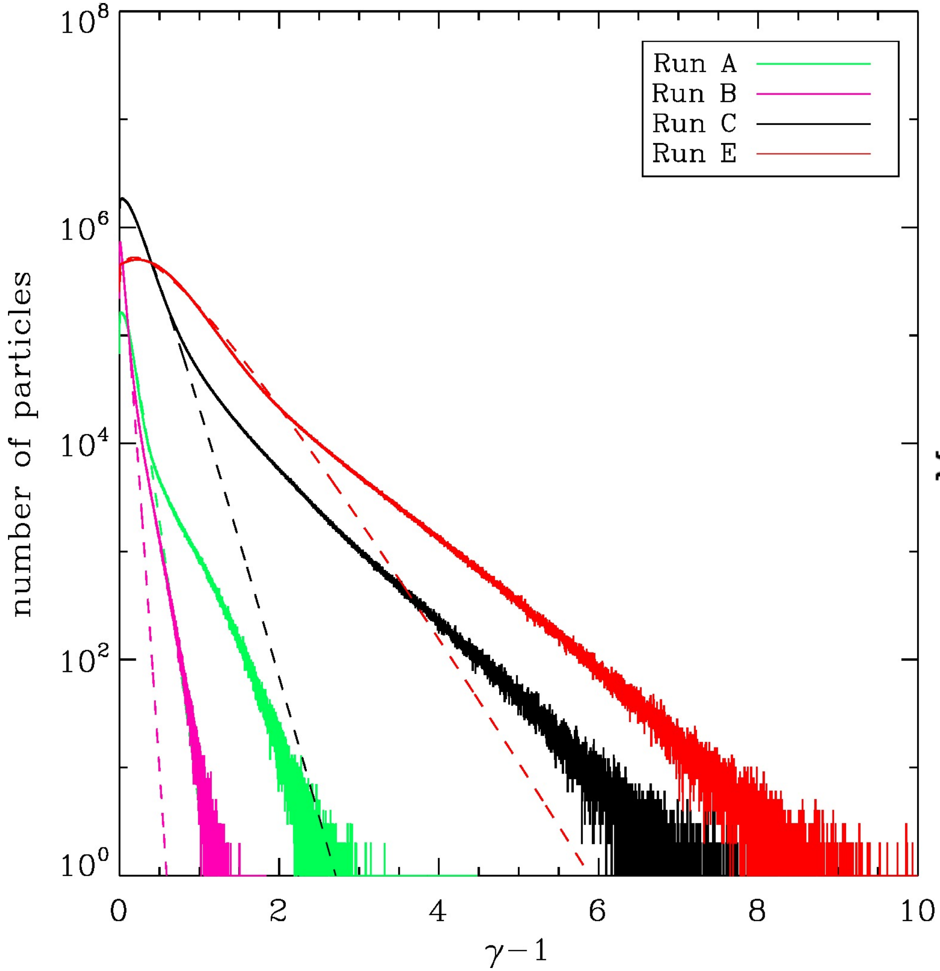

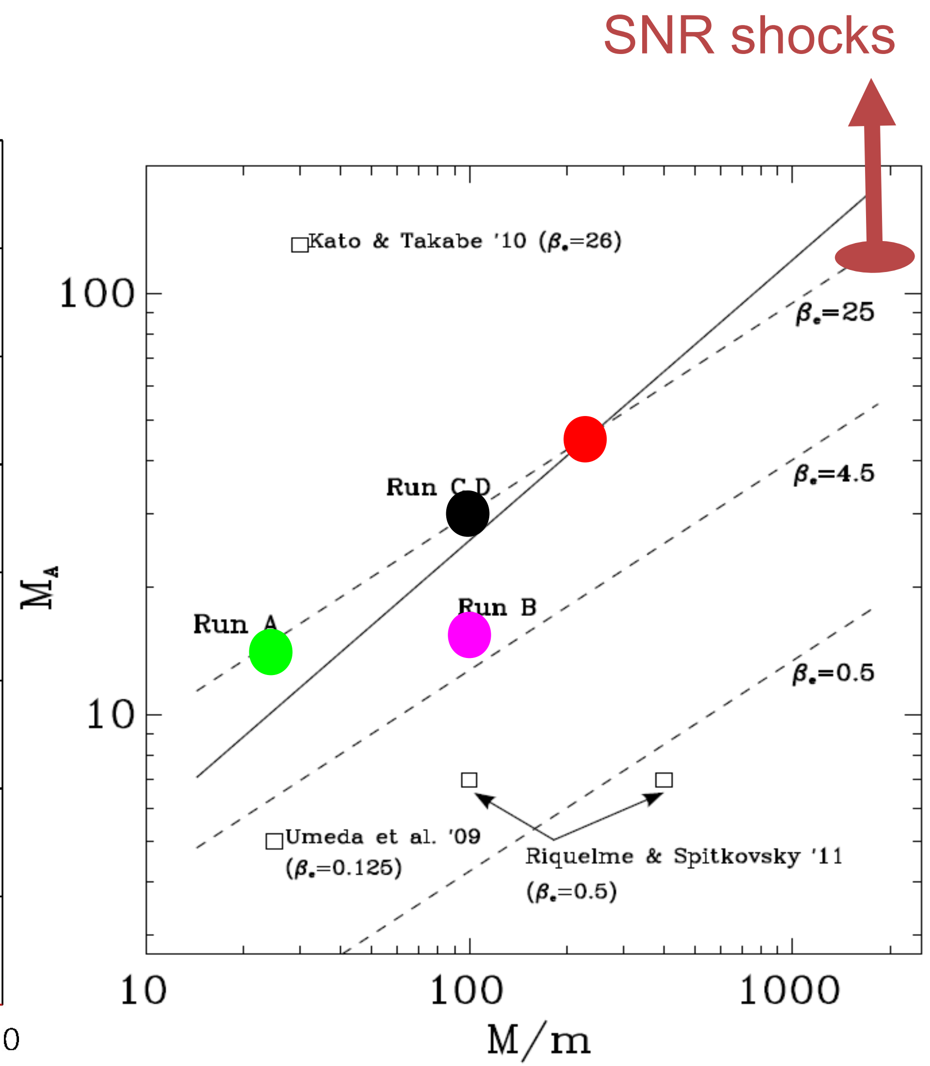

Matsumoto+ '12, '13

Physics in high M_A shocks

out-of-plane field

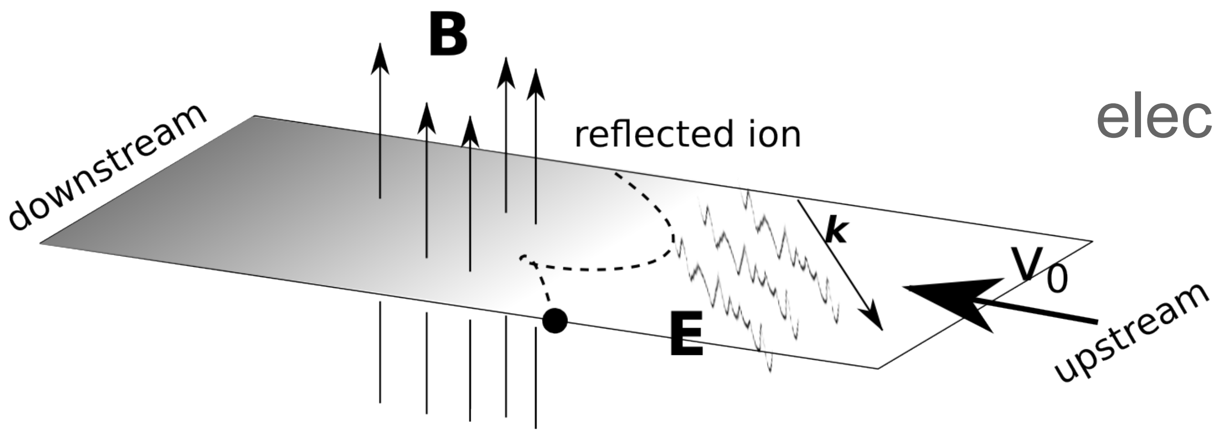

k perp $\mathbf{B}_0$

elecron pre-acceleration

in-plane field

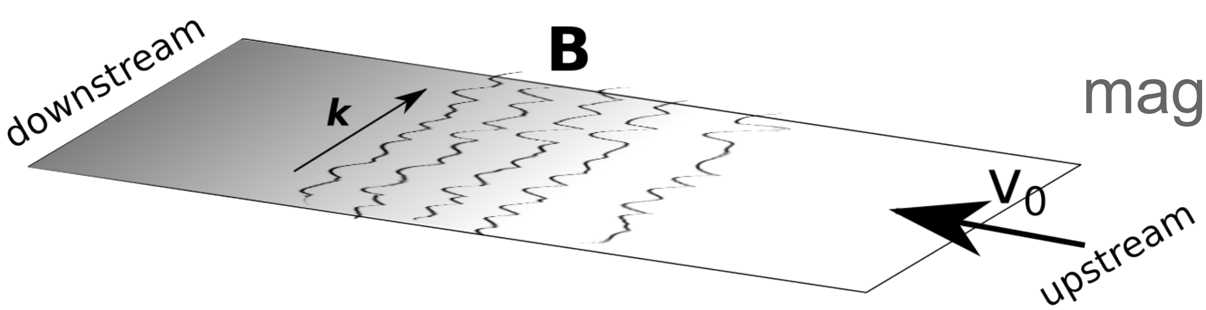

k // $\mathbf{B}_0$

magnetic field turbulence

In-plane **B** field case

M_A~5

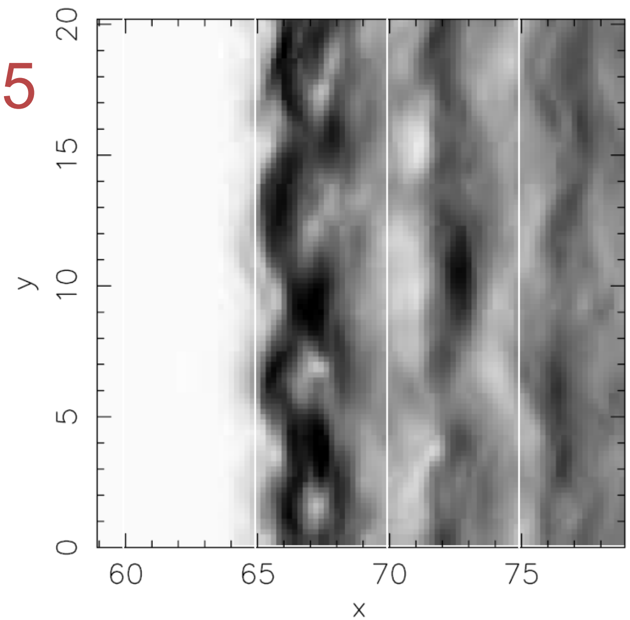

- Ion-scale ripples along the shock surface
- Ion cycrotron-instability
- Ion-beam Weibel instability
- Origin of ion-scale magnetic field turbulence

Burgess, '06

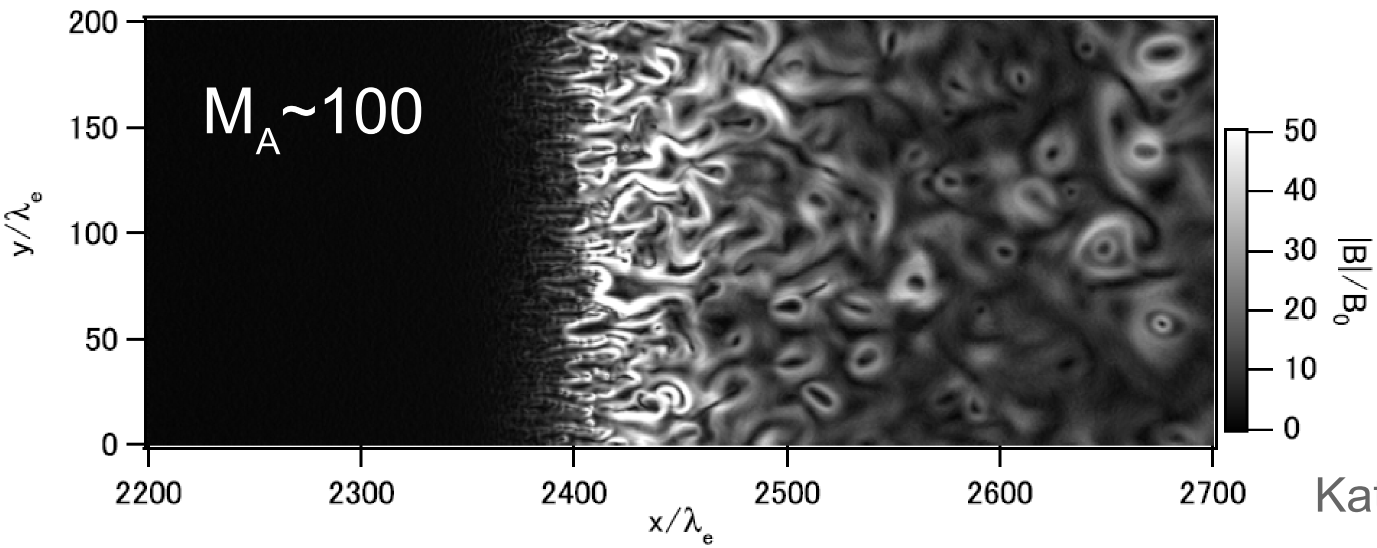

Kato & Takabe, '11

Stochastic accel. at M/m=225, M_A~42 shock

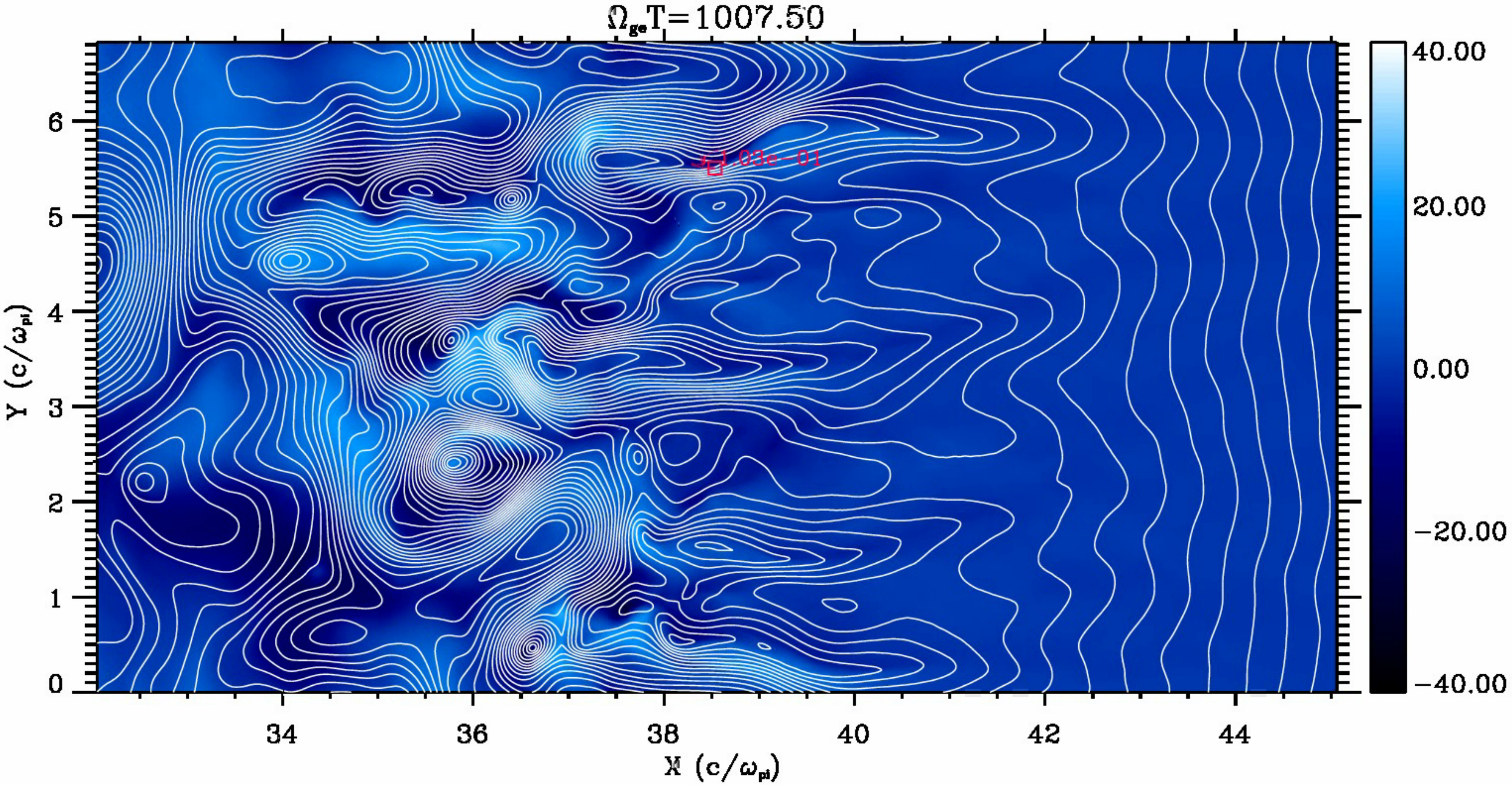

blue: Bz component, white: in-plane **B** field lines, red: electron orbit

Electron accelerations in perp. shocks

Trapping condition

Linear unstable condition

young SNR shocks

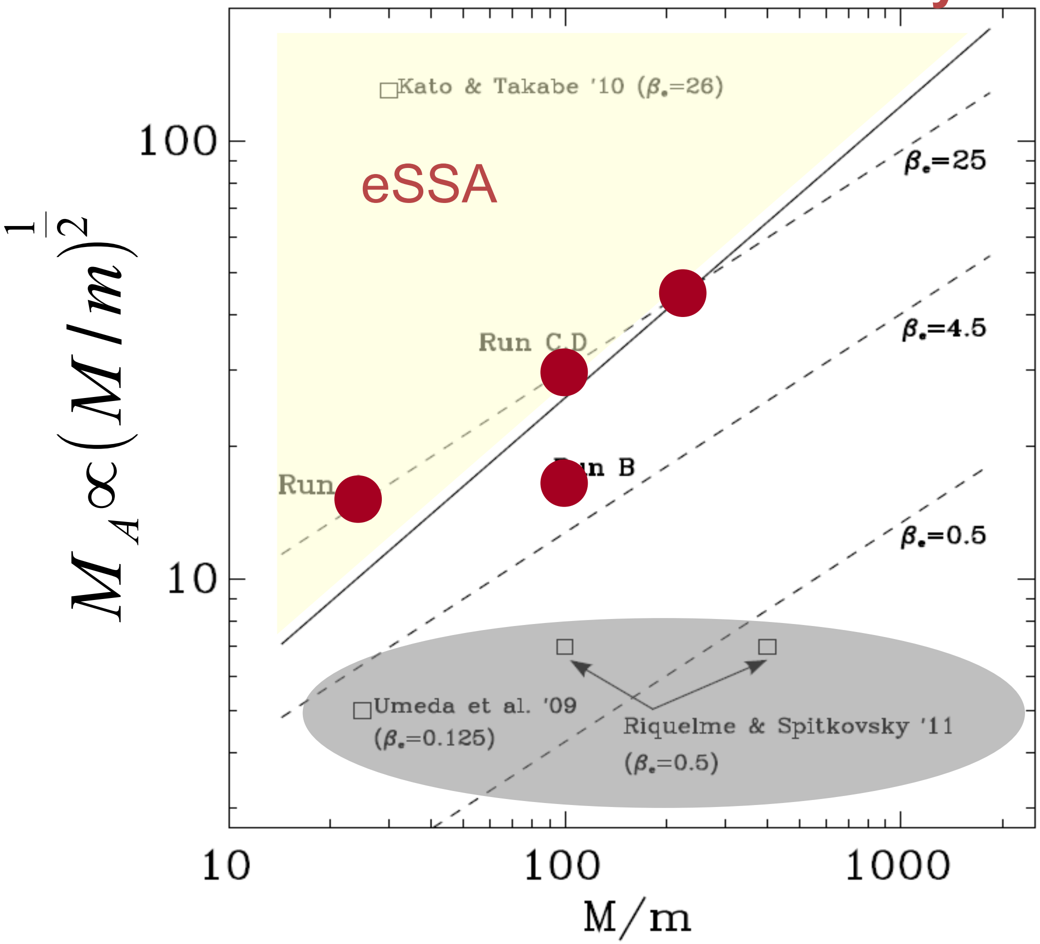

Whistler wave

Electron accelerations in perp. shocks

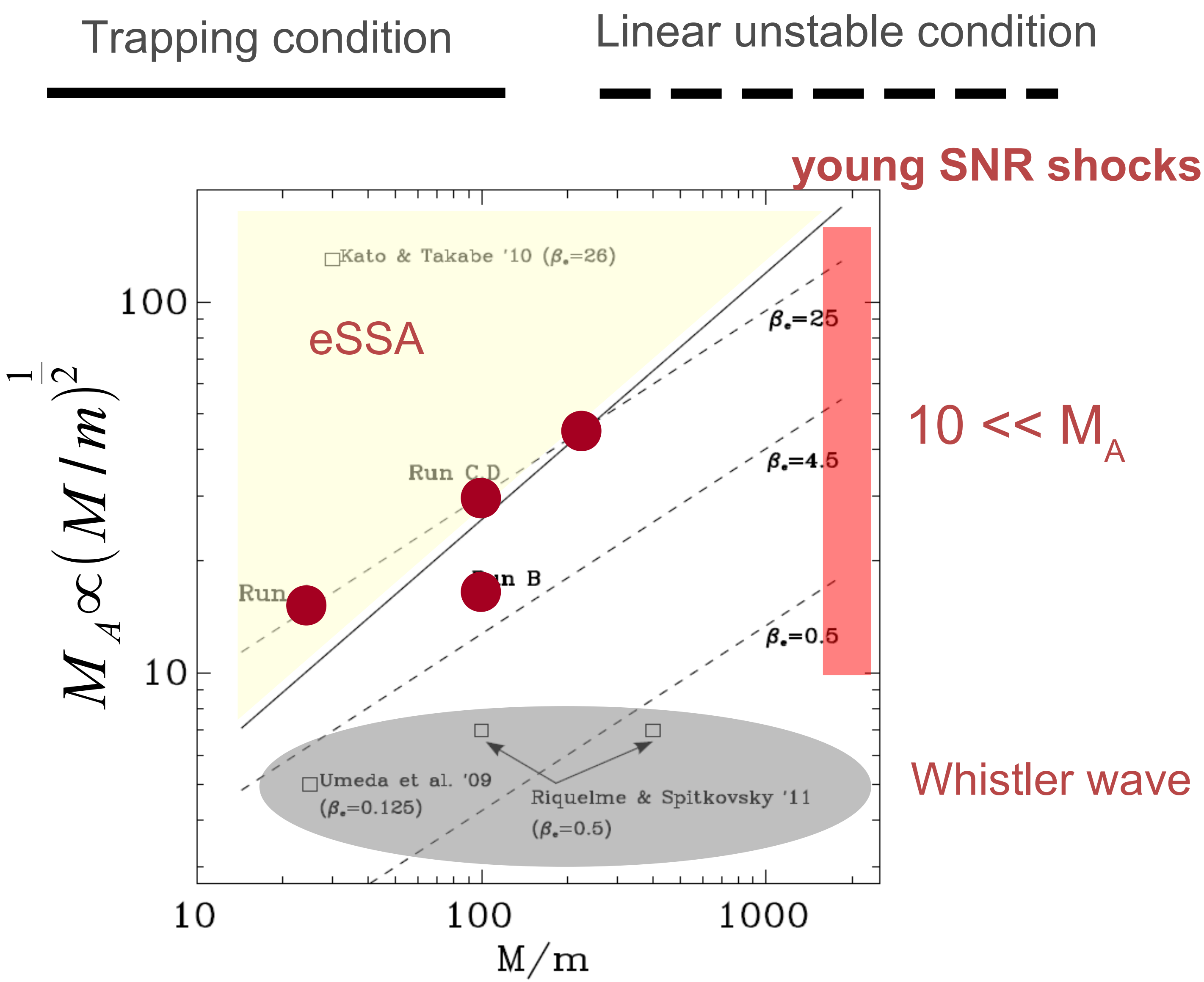

Physics in high M_A shocks

out-of-plane field

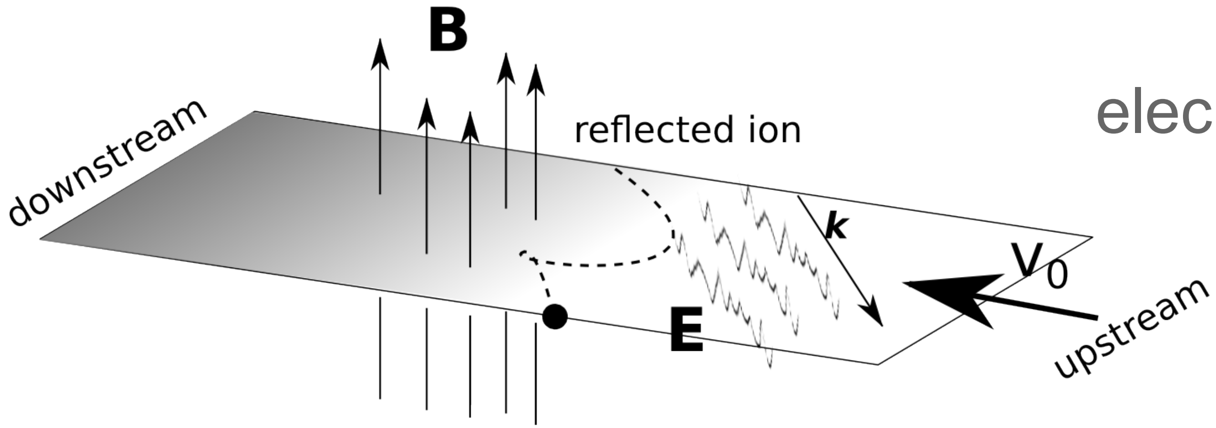

k perp $\mathbf{B_0}$

elecron pre-acceleration

in-plane field

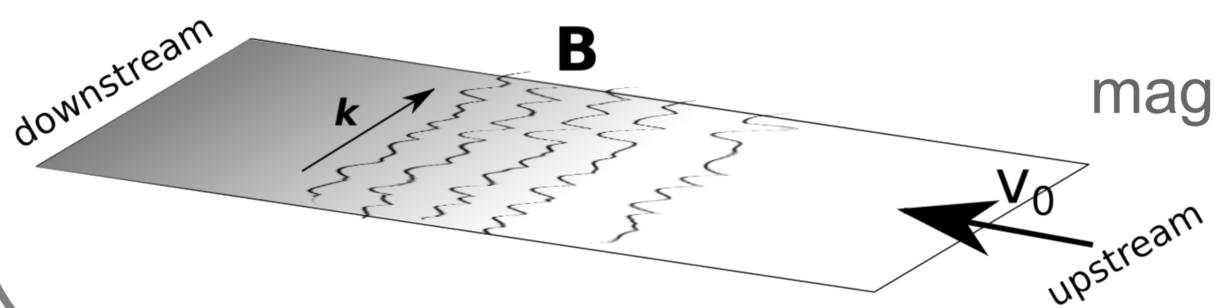

k // $\mathbf{B_0}$

magnetic field turbulence

Trillion-particle simulations on 京 K computer

- 3D PIC simulation of a quasi-perpendicular shock
- $M/m=64$, $M_A \sim 24$ ($v_{sh} \sim 0.3c$)
- $(N_x, N_y, N_z) = (8000, 768, 768)$
- 10^{12} particles (~ 100 /cell)
- On 9216 nodes (73,728 cores)
- 50 TB for a snapshot
- The largest-scale shock experiments!

Preliminary result (ongoing)

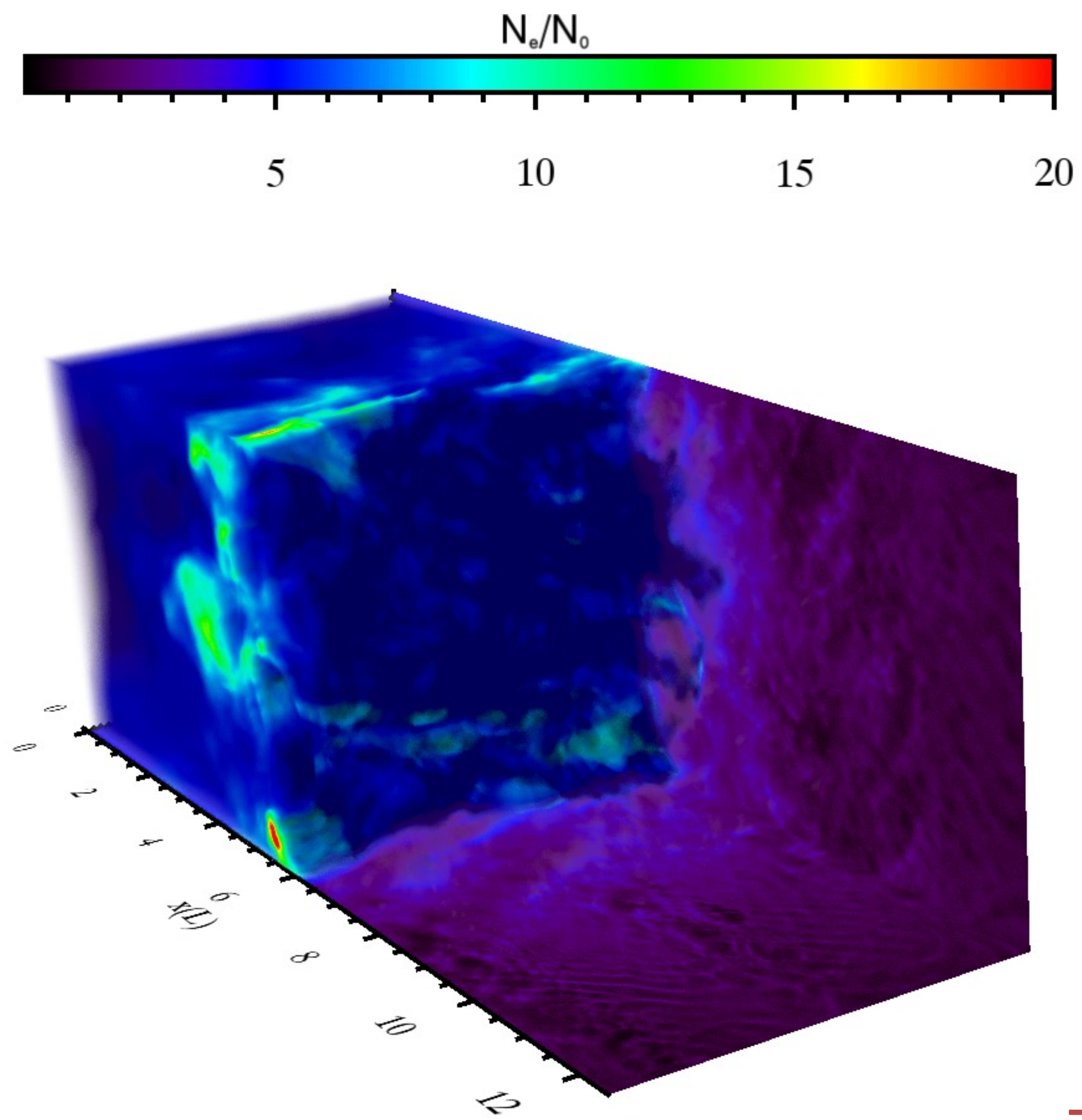

Thank you